Analysis of Downlink Connectivity Models in a Heterogeneous Cellular Network via Stochastic Geometry

Prasanna Madhusudhanan, Juan G. Restrepo, Youjian Liu, *Member, IEEE*, and Timothy X Brown

***Abstract*—In this paper, a comprehensive study of the downlink performance in a heterogeneous cellular network (or HetNet) is conducted via stochastic geometry. A general HetNet model is considered consisting of an arbitrary number of open-access and closed-access tiers of base stations (BSs) arranged according to independent homogeneous Poisson point processes. The BSs within each tier have a constant transmission power, random fading factors with an arbitrary distribution and arbitrary path-loss exponent of the power-law path-loss model. For such a system, analytical characterizations for the coverage probability are derived for the max-SINR connectivity and nearest-BS connectivity models. Using stochastic ordering, interesting properties and simplifications for the HetNet downlink performance are derived by relating these two connectivity models to the maximum instantaneous received power (MIRP) connectivity model and the maximum biased received power (MBRP) connectivity models, providing good insights about HetNets and their downlink performance in these complex networks. Furthermore, the results also demonstrate the effectiveness and analytical tractability of the stochastic geometric approach to study the HetNet performance.**

***Index Terms*—Multi-tier networks, Cellular Radio, Co-channel Interference, Fading channels, Poisson point process, max-SINR connectivity, nearest-BS connectivity.**

I. Introduction

THE MODERN cellular communication network is an overlay of multiple contributing subnetworks such as the macrocell, microcell, picocell and femtocell networks. These are denoted collectively as heterogeneous networks (or, in short, *HetNets*). HetNets have been shown to sustain greater end-user data-rates as well as provide indoor and cell-edge coverage. As such, they are an important feature of fourth-generation (4G) cellular standards [4]–[10].

Until recently, such networks have been analyzed solely through system simulations. HetNets consist of regularly spaced macrocell base-stations (BSs) along with irregularly spaced microcell and picocell BSs and randomly placed end-user deployed femtocell BSs. The BSs in each of these networks have different transmission powers and radio environments. Some BSs (e.g. a customer's femtocell in their home) may accept only a private subset of users. These BSs are essentially interference sources for other users. Some HetNets may operate among unlicensed or secondary devices that are also interference sources. The result is a complex environment with many parameters that cannot be efficiently studied through simulation. Under these circumstances, an analytical model that captures all the design scenarios of interest is needed.

Cellular networks modeled with randomly deployed nodes have yielded a rich set of results [11]–[14]. An important tool in this work is the homogeneous Poisson point process [15]–[17]. It can yield analytically tractable results unlike purely simulation-based studies based on a regular hexagonal grid [18]–[20]. In practice, we observe that increasingly dense and irregular BS deployments deviate significantly from an ideal regular grid. Further, studies have shown that increasing radio variability drives the performance of ideal regularly spaced BSs to that of BSs deployed as a homogeneous Poisson point process [16, Fig. 2], [21, Theorem 3].

In light of the above motivations, it is well-justified to study a HetNet composed of multiple tiers of networks (e.g. macrocell, microcell, picocell and femtocell networks), each modeled as an independent homogeneous Poisson point process. Such studies have been done in [22]–[30] and by us in [1]–[3]. These studies mathematically characterize important performance metrics such as the signal-to-interference-plus-noise ratio (SINR) distribution, coverage probability (1 - outage probability), average ergodic rate, and average load carried by BSs of each tier.

In this paper we focus on the HetNets downlink coverage probability. The main contribution is to develop a general framework that combines and extends these existing results. We consider BSs assigned to different tiers. Each tier is a homogeneous set of radios deployed as a Poisson point process with common transmission, propagation, fading factor, and

Manuscript received May 26, 2015; revised November 18, 2015; accepted January 23, 2016. Date of publication March 31, 2016; date of current version June 7, 2016. This work was supported by the NSF under Grant ECCS-1408604 and Grant IIP-1414250. Special cases of the results in this paper were presented in [1]–[3]. The associate editor coordinating the review of this paper and approving it for publication was M. Bennis.

P. Madhusudhanan was with the Department of Electrical, Computer, and Energy Engineering, University of Colorado Boulder, Boulder, CO 80309-0425 USA. He is now with Qualcomm Inc., Boulder, CO 80301 USA (e-mail: mprasanna@colorado.edu).

J. G. Restrepo is with the Department of Applied Mathematics, University of Colorado Boulder, Boulder, CO 80309-0526 USA (e-mail: juanga@colorado.edu).

Y. Liu is with the Department of Electrical, Computer, and Energy Engineering, University of Colorado Boulder, Boulder, CO 80309-0425 USA (e-mail: eugeneliu@ieee.org).

T. X Brown is with the Interdisciplinary Telecom Program and Department of Electrical, Computer, and Energy Engineering, University of Colorado Boulder, Boulder, CO 80309-0425 USA, and also with Electrical and Computer Engineering, Carnegie Mellon University, Pittsburgh, PA 15213 USA (e-mail: timxb@colorado.edu).

Color versions of one or more of the figures in this paper are available online at http://ieeexplore.ieee.org.

Digital Object Identifier 10.1109/TWC.2016.2530723

reception parameters. Different tiers may have different densities and radio parameters. Results on this model can be distinguished along two dimensions. The first is the algorithm used to select which BS a mobile station (MS) connects. Different connectivity models will be defined later and include max-SINR, nearest BS, maximum biased received power (MBRP), and maximum instantaneous received power (MIRP). A second dimension is which of the radio parameters are allowed to vary between tiers.

The tiers can be further classified as open-access or closed-access [3], [26], [25], [31]. Open-access tiers consist of ordinary BSs to which any MS can connect. Closed-access tiers represent private femtocells, unlicensed devices, and other interference sources. Whether they consist of actual BSs or not, closed-access tiers model interfering radios that do not provide service to the MS we wish to study. The open and closed-access tiers enable many flexible HetNet models to be developed. A simple model might consist of two tiers. One open-access tier consists of tall long-range macrocell BS towers with appropriate radio parameters. A second closed-access tier consists of low-power indoor femtocells with corresponding radio parameters. A more complex model might segregate BSs into many finely distinguished tiers to represent different types of operator equipment and interference sources.

The max-SINR connectivity model where the fading factors are exponentially distributed and the path-loss exponents are the same for all tiers was considered in [26], [27]. Using an entirely different approach, [22]–[24] derives the coverage probability for the HetNet with max-SINR and nearest BS connectivity models, and exponentially distributed fading factors. In [30], the authors study the HetNet coverage probability for MBRP connectivity, and, again, for the exponentially distributed fading. In [1]–[3], we studied the HetNet coverage probability and stochastic ordering results for MIRP connectivity in the case when the fading factors have an arbitrary distribution and each tier's path-loss exponent may differ.

In this paper we consider nearest-BS and max-SINR connectivity models as a natural extension of our earlier results to popular connectivity models. We derive the coverage probabilities when each tier has arbitrary transmit power, fading factor distribution, path loss exponent, and receiver SINR threshold. The result is a relatively complex semi-analytic expression. This is found to be useful in several ways. First we are able to make a qualitative study of performance using results from stochastic ordering. We show that MBRP and MIRP connectivity models are a special case of nearest-BS and max-SINR connectivity models, respectively. We also derive a reduced canonical form for the HetNets that can, in some cases, simplify the HetNet to an equivalent network with one or a few tiers. When the SINR thresholds of all the tiers are above 1, we show the HetNet coverage probability under max-SINR connectivity and MIRP connectivity are identical, and nearest-BS connectivity and the MBRP connectivity are identical. Further, in these special cases, simple and novel analytical expression are derived for the coverage probability, average rate and the load carried by the BSs of each tier. Finally, the semi-analytic expression is used to study a specific two-tier example. We start with the system model.

II. System Model

This section describes the various elements used to model the wireless network: the BS layout, the radio environment, and the role of the BS connectivity model.

A. BS Layout

The HetNet is composed of K open-access and L closed-access tiers. The BS layout in each tier is according to an independent homogeneous Poisson point process in $\mathbb{R}^2$ with density $\lambda_{ok}, \lambda_{cl}$ for the k^{th} open-access tier and l^{th} closed-access tier, respectively, where $k = 1, \ldots, K$ and $l = 1, \ldots, L$. The MS is allowed to communicate with any BS of the open-access tiers, but cannot communicate with any of the closed-access BSs. We assume the MS location is independent of the BS locations. Since the BS densities are homogeneous, without loss of generality, the MS is placed at the origin.

B. Radio Environment and Downlink SINR

The signal transmitted from each BS undergoes fading and path-loss. At this point we do not concern ourselves whether the fading is fast fading or slow (shadow) fading and refer to it as a generic fading factor. The SINR at an arbitrary MS in the system from the i^{th} BS of the k^{th} open-access tier is the ratio of the received power from this BS to the sum of the interferences from all the other BSs in the system and the constant background noise η, and is expressed as

$$\text{SINR}_{ki} = \frac{P_{ok}\Psi_{oki}R_{oki}^{-\varepsilon_{ok}}}{I_o - P_{ok}\Psi_{oki}R_{oki}^{-\varepsilon_{ok}} + I_c + \eta}, \tag{1}$$

where subscripts 'o' and 'c' indicate open-access and closed-access tiers, respectively, $I_o = \sum_{m=1}^{K}\sum_{n=1}^{\infty} P_{om}\Psi_{omn}R_{omn}^{-\varepsilon_{om}}$ is the sum of the received powers from all the open-access tier BSs; $\{P_{om}, \Psi_{omn}, \varepsilon_{om}, R_{omn}\}_{m=1,\, n=1}^{m=K,\, n=\infty}$ are the constant transmit power, random fading factor, constant path-loss exponent, and the distance from the MS to the n^{th} nearest BS of the m^{th} open-access tier; $I_c = \sum_{l=1}^{L}\sum_{n=1}^{\infty} P_{cl}\Psi_{cln}R_{cln}^{-\varepsilon_{cl}}$ is the sum of the received powers from all the closed-access tier BSs; $\{P_{cl}, \Psi_{cln}, \varepsilon_{cl}, R_{cln}\}_{l=1,\, n=1}^{l=L,\, n=\infty}$ lists the constant transmit power, random fading factor, the constant path-loss exponent, and the distance from the MS to the n^{th} nearest BS of the l^{th} closed-access tier. The fading factors $\{\Psi_{omn}\}_{n=1}^{\infty}$ are i.i.d. random variables with the same distribution as Ψ_{om}, $m = 1, \ldots, K$, and similarly, the fading factors $\{\Psi_{cln}\}_{n=1}^{\infty}$ are i.i.d. random variables with the same distribution as Ψ_{cl}, $l = 1, \ldots, L$. Further, following [19], it is assumed that $\left\{\mathbb{E}\left[\Psi_{om}^{\frac{2}{\varepsilon_m}}\right]\right\}_{m=1}^{K}$, $\left\{\mathbb{E}\left[\Psi_{cl}^{\frac{2}{\varepsilon_{cl}}}\right]\right\}_{l=1}^{L} < \infty$. The various symbols introduced in this section are listed in Table I for quick reference.

C. BS Connectivity Models

Given thresholds $\{\beta_k\}_{k=1}^{K}$, a MS is able to communicate with a BS i of the k^{th} open-access tier if $\text{SINR}_{ki} > \beta_k$. In this case,

the MS is said to be in *coverage*. The BS connectivity model determines to which BS the MS connects and consequently its coverage performance. The next two sections provide the main results of this paper. They define and analyze the max-SINR, nearest-BS, MIRP, and MBRP connectivity models.

III. Max-SINR and Nearest-BS Coverage Probability

Under the max-SINR connectivity model, the MS is said to be in coverage if there exists at least one BS among all the open-access tiers with an SINR at the MS above the corresponding threshold, and is expressed as follows.

$$\mathbb{P}_{\text{coverage}}^{\text{max-SINR}} = \mathbb{P}\left(\bigcup_{k=1}^{K}\left\{\max_{i}\left(\text{SINR}_{ki}\right) > \beta_k\right\}\right), \tag{2}$$

where SINR_{ki} corresponds to the SINR of the i^{th} BS of the k^{th} tier as defined in (1).

The MS is said to be in coverage under the nearest-BS connectivity model if there exists at least one of the nearest BSs of the K open-access tiers with SINR at the MS above the corresponding threshold. This is expressed as

$$\mathbb{P}_{\text{coverage}}^{\text{nearest}} = \mathbb{P}\left(\bigcup_{k=1}^{K}\left\{\text{SINR}_{k1} > \beta_k\right\}\right), \tag{3}$$

where SINR_{k1} is the SINR at the MS from tier k's nearest BSs. The relative performance is given in this proposition.

Proposition 1: For the same system parameters, $\mathbb{P}_{\text{coverage}}^{\text{max-SINR}} \geq \mathbb{P}_{\text{coverage}}^{\text{nearest}}$.

The above result is easily proved by noting the coverage events in (2) are a superset of those in (3).

The downlink coverage probability under max-SINR connectivity for a single-tier network was computed in [14]. The method is generalized to compute the coverage probability for the max-SINR and nearest-BS connectivity models for the more general HetNets model.

Theorem 1: The HetNet coverage probability under the max-SINR and the nearest-BS connectivity models are as follows:

$$\begin{aligned}\mathbb{P}_{\text{coverage}}^{\text{max-SINR}} = &\sum_{i=1}^{K}\lambda_{oi}\frac{2\pi}{\varepsilon_{oi}}\left(\gamma_i P_{oi}\right)^{\frac{2}{\varepsilon_{oi}}}\mathbb{E}\left[\Psi_{ok}^{\frac{2}{\varepsilon_{ok}}}\right]\\ &\times\int_{y=0}^{\infty}\int_{\omega=-\infty}^{\infty}\mathcal{L}_{I_o+I_c+\eta,\ \max\limits_{i=1,\cdots,K}\gamma_i M_i\leq y}\left(j\omega\right)\\ &\times\frac{\left(\mathrm{e}^{j\omega y\left(1-\gamma_i^{-1}\right)}-\mathrm{e}^{j\omega\left(\eta+y\left(\kappa^{-1}-\gamma_i^{-1}\right)\right)}\right)}{2\pi j\omega y^{1+\frac{2}{\varepsilon_{oi}}}}d\omega dy,\end{aligned} \tag{4}$$

$$\begin{aligned}\mathbb{P}_{\text{coverage}}^{\text{nearest}} = &\int_{y=0}^{\infty}\int_{\omega=-\infty}^{\infty}\frac{\mathrm{e}^{j\omega y}-\mathrm{e}^{j\omega\left(\frac{y}{\kappa}+\eta\right)}}{j\omega 2\pi}\\ &\times\frac{\partial}{\partial u}\mathcal{L}_{I_o+I_c+\eta,\ \max\limits_{i=1,\cdots,K}\gamma_i N_i\leq u}\left(j\omega\right)\Big|_{u=y}d\omega dy,\end{aligned} \tag{5}$$

TABLE I
List of Symbols Used in the Paper

Symbol	Description
$K,\ L$	Number of open- and closed-access tiers
$\{\lambda_{ok}\}_{k=1}^{K},\{\lambda_{cl}\}_{l=1}^{L}$	BS densities of open- and closed-access tiers
$\{P_{ok}\}_{k=1}^{K},\{P_{cl}\}_{l=1}^{L}$	Constant BS transmission powers
$\{\varepsilon_{ok}\}_{k=1}^{K},\{\varepsilon_{cl}\}_{l=1}^{L}$	Path-loss exponents ($\varepsilon > 2$)
$\{\Psi_{ok}\}_{k=1}^{K},\{\Psi_{cl}\}_{l=1}^{L}$	random fading factors $\left(\mathbb{E}\left[\Psi^{\frac{2}{\varepsilon}}\right] < \infty\right)$
$\{\beta_k\}_{k=1}^{K}$	SINR connectivity thresholds
$\{B_k\}_{k=1}^{K}$	Tier bias values in MBRP connectivity
η	Background noise power
$I_o,\ I_c$	Total received power from open, closed tiers
$\{\gamma_k\}_{k=1}^{K}$	$\triangleq\left\{1+\frac{1}{\beta_k}\right\}_{k=1}^{K}$

where $\kappa = \max\limits_{i=1,\cdots,K}\gamma_i$ (see Table I); and the Laplace transform function, $\mathcal{L}_{I_o+I_c+\eta,\ \max\limits_{i=1,\cdots,K}\gamma_i M_i\leq y}\left(j\omega\right)$, in (4) and the derivative of the Laplace transform function, $\frac{\partial}{\partial u}\mathcal{L}_{I_o+I_c+\eta,\ \max\limits_{i=1,\cdots,K}\gamma_i N_i\leq u}\left(j\omega\right)$, in (5) are given in (30) and (35), respectively.

Proof: See Appendix A. ■

Using an alternate approach, expressions for the HetNet coverage probability are obtained in [22] when all the fading factors are i.i.d. exponential random variables. For a general system model as in this paper, to the best of our knowledge, the HetNet coverage probability has not been characterized before.

The semi-analytical expressions are extremely complicated even for numerical computations. Nevertheless, we can gain some insights into the problem. First, we observe the role of fading in the max-SINR connectivity model.

Corollary 1: The HetNet performance under max-SINR connectivity with an arbitrary fading distribution at each tier is the same as in another HetNet with open-access and closed-access BS densities as $\left\{\lambda_{oi}\mathbb{E}\left[\Psi_{oi}^{\frac{2}{\varepsilon_{oi}}}\right]\right\}_{i=1}^{K}$ and $\left\{\lambda_{ci}\mathbb{E}\left[\Psi_{ci}^{\frac{2}{\varepsilon_{ci}}}\right]\right\}_{i=1}^{L}$, respectively, and unit fading factor.

The above result is obtained by noting that the effect of fading is equivalent to scaling the density of BSs by the $\frac{2}{\varepsilon}^{\text{th}}$ moment of the fading factor random variable [19, Corollary 2]. Most prior wireless network studies that use stochastic geometry assume fading factors to be i.i.d. exponential random variables, as this greatly simplifies the analysis and renders itself to closed-form coverage probabilities and other related performance metrics (see [26]). However, the exponential distribution does not accurately capture the slow fading environment. Interestingly, the above corollary shows any fading factor distribution that has the correct $\frac{2}{\varepsilon}^{\text{th}}$ moment is sufficient for the max-SINR connectivity model. Unfortunately, the same is not true for the nearest-BS connectivity model.

Next, we observe that we only ever need to consider a single closed tier of BSs with unity transmission power and fading factor.

Corollary 2: If the closed tier path-loss exponents are all equal, i.e. $\{\varepsilon_{cl}\}_{l=1}^{L} = \varepsilon_c$, the downlink coverage probability in

the HetNet is the same as in another HetNet with the same open-access tiers as in the original HetNet (described in Section II-A) and one closed access tier where the BSs have unity transmission power and fading factor, and are arranged according to a homogeneous Poisson point process with a BS density given by $\lambda_c = \sum_{l=1}^{L} \lambda_{cl} P_{cl}^{\frac{2}{\varepsilon_c}} \mathbb{E}\left[\Psi_{cl}^{\frac{2}{\varepsilon_c}}\right]$.

Proof: Inspecting equations (4), (5), (29)–(31) the closed-access tiers affect the HetNet downlink coverage probability solely through the Laplace transform expression in (29). Substituting $\{\varepsilon_{cl}\}_{l=1}^{L} = \varepsilon_c$ in (29), the Laplace transform is the same as in the case when there is a single closed-access tier with base-station arrangement according to a homogeneous Poisson point process with BS density λ_c, unity transmission power and fading factor, and path-loss exponent ε_c. ■

When the path-loss expoenents differ between closed tiers, we can still create a single equivalent closed tier but with a non-homogeneous intensity function as follows.

Corollary 3: The downlink coverage probability in the HetNet is the same as in another HetNet with the same open-access tiers as in the original HetNet (described in Section II-A) and one closed access tier where the BSs have unity transmission power, fading factor and path-loss exponent, and are arranged according to a non-homogeneous Poisson point process with a BS density as a function of radial distance r from the origin:

$$\lambda_c(r) = \sum_{l=1}^{L} \lambda_{cl} P_{cl}^{\frac{2}{\varepsilon_{cl}}} \mathbb{E}\left[\Psi_{cl}^{\frac{2}{\varepsilon_{cl}}}\right] r^{\frac{2}{\varepsilon_{cl}}-1}, \; r \geq 0. \tag{6}$$

Proof: The total closed-access interference power I_c is independent of the signal power and interference power at the MS from the open-access tiers. Next, I_c satisfies the following stochastic equivalence $I_c =_{\text{st}} \sum_{n=1}^{\infty} \tilde{R}_n^{-1}$, where $\left\{\tilde{R}_n\right\}_{n=1}^{\infty}$ is the set of distances from the origin of BSs arranged according to a non-homogeneous Poisson point process with BS density function given in (6). This is obtained by first using [19, Theorem 2] to obtain an equivalent BS arrangement for each closed-access tier according to non-homogeneous Poisson point process with unity transmission power, fading factor and path-loss exponent at each BS in the tier. Since the BS arrangements, transmission and fading characteristics of the BSs of all closed-access tiers are independent of each other, using the Superposition theorem [32, Page 16], the L closed-access tiers can be combined together to obtain a single closed-access tier with BS density function as shown in (6). Due to [19, Theorem 2], the equivalent BS arrangement has the same probability distribution for I_c as the original case. ■

We note that both corollaries apply to the max-SINR and nearest-BS connectivity models.

IV. MIRP and MBRP Coverage Probability

Under the maximum instantaneous received power (MIRP) connectivity model, the MS connects to the BS with the maximum instantaneous received power among all the open-access tiers. This BS will also have the highest SINR (since all tiers contribute to the interference). Let this BS's index be $(T, I) = \underset{k=1,\cdots,\, K,\; i=1,\, 2,\cdots}{\text{argmax}} \text{SINR}_{k,i}$. In this case

$$\mathbb{P}_{\text{coverage}}^{\text{MIRP}} = \mathbb{P}\left(\left\{\text{SINR}_{T,I} > \beta_T\right\}\right) \tag{7}$$

Another HetNet connectivity model is the maximum biased received power (MBRP) connectivity model studied in [30]. Under MBRP, the MS associates with the BS with the maximum long-term average received-power with a certain bias in each tier. By long-term average we mean the MS measures the expected value of the fading factor. Since fading factors within a tier all have the same distribution, the serving BS will be the nearest BS in its tier. The tier-index of the serving BS and the HetNet coverage probability under MBRP are determined as follows:

$$\begin{aligned} T &= \underset{k=1,\cdots,\, K}{\text{argmax}} \; \max_{i=1,\, 2,\cdots} P_{ok} \mathbb{E}\left[\Psi_{oki}\right] R_{oki}^{-\varepsilon_{ok}} B_{ok} \\ &= \underset{k=1,\cdots,\, K}{\text{argmax}} \; P_{ok} \mathbb{E}\left[\Psi_{ok}\right] R_{ok1}^{-\varepsilon_{ok}} B_{ok} \end{aligned} \tag{8}$$

$$\mathbb{P}_{\text{coverage}}^{\text{MBRP}} = \mathbb{P}\left(\left\{\text{SINR}_{T,1} > \beta_T\right\}\right), \tag{9}$$

where $\{B_{ok}(>0)\}_{k=1}^{K}$ are the biasing factors; $\left\{P_{ok}\mathbb{E}\left[\Psi_{oki}\right] R_{oki}^{-\varepsilon_{ok}}\right\}_{i=1}^{\infty}$ is the long-term averaged received power at the MS from the k^{th} tier BSs; and $\text{SINR}_{k,i}$ is defined in (1). When $\{B_{ok}\}_{k=1}^{K} = 1$, MBRP is called maximum averaged received power (MARP) connectivity.

From the definition of the HetNet coverage probability under MIRP and MBRP, the stochastic ordering result can be extended beyond Proposition 1 as follows.

Proposition 2: If a HetNet has $\{\beta_k\}_{k=1}^{K} = \beta$ or $\{\beta_k\}_{k=1}^{K} \geq 1$, and the MBRP bias factor is $B_{ok} = \frac{1}{P_{ok}\mathbb{E}[\Psi_{ok}]}$ for $k = 1, \cdots, K$, then $\mathbb{P}_{\text{coverage}}^{\text{MBRP}} = \mathbb{P}_{\text{coverage}}^{\text{nearest}} \leq \mathbb{P}_{\text{coverage}}^{\text{max-SINR}} = \mathbb{P}_{\text{coverage}}^{\text{MIRP}}$.

Proof: With $B_{ok} = \frac{1}{P_{ok}\mathbb{E}[\Psi_{ok}]}$, for $k = 1, \cdots, K$, by inspecting equations (8), (9) and (26), we get $\mathbb{P}_{\text{coverage}}^{\text{MBRP}} = \mathbb{P}_{\text{coverage}}^{\text{nearest}}$. When $\{\beta_k\}_{k=1}^{K} = \beta$, by inspecting equations (7) and (25), it is clear that $\mathbb{P}_{\text{coverage}}^{\text{max-SINR}} = \mathbb{P}_{\text{coverage}}^{\text{MIRP}}$. From [26, Lemma 1], when $\{\beta_k\}_{k=1}^{K} \geq 1$, there exists at most one open-access BS that can have an SINR above the corresponding threshold. As a result, HetNet coverage probability in (2) becomes $\mathbb{P}_{\text{coverage}}^{\text{max-SINR}} = \sum_{k=1}^{K} \mathbb{P}\left(\{\max_i \left(\text{SINR}_{ki}\right) > \beta_k\}\right) = \mathbb{P}_{\text{coverage}}^{\text{MIRP}}$. ■

For the remainder of this section, we assume a single closed access tier with homogeneous intensity λ_c, transmission power P_c, path-loss exponent ε_c and i.i.d. fading factors Ψ_c $\left(\mathbb{E}\left[\Psi_c^{\frac{2}{\varepsilon_c}}\right] < \infty\right)$. We begin by analyzing the MIRP case.

A. SINR Characterization Under MIRP Connectivity

The SINR characterization is simplified by considering a stochastically equivalent two-tier 1-D system as follows.

Lemma 1: The SINR at the MS under MIRP is the same as in a one-dimensional non-homgeneous two-tier HetNet with one open-access network and one closed-access network, respectively. In the equivalent two-tier HetNet, the open-access network has a BS density function $\tilde{\lambda}(r) = \sum_{k=1}^{K} \tilde{\lambda}_{ok}(r)$

with $\tilde{\lambda}_{ok}(r) = \lambda_{ok}\frac{2\pi}{\varepsilon_{ok}} P_{ok}^{\frac{2}{\varepsilon_{ok}}} \mathbb{E}\left[\Psi_{ok}^{\frac{2}{\varepsilon_{ok}}}\right] r^{\frac{2}{\varepsilon_{ok}}-1}$, $r \geq 0$ and the closed-access network has a BS density function $\hat{\lambda}(r) = \lambda_c \frac{2\pi}{\varepsilon_c} P_c^{\frac{2}{\varepsilon_c}} \mathbb{E}\left[\Psi_c^{\frac{2}{\varepsilon_c}}\right] r^{\frac{2}{\varepsilon_c}-1}$. All the BSs in the equivalent HetNet have unity transmit powers, fading factors and path-loss exponents. The SINR stochastic equivalence is shown below

$$\mathrm{SINR}_{T,I} =_{\mathrm{st}} \frac{\tilde{R}_1^{-1}}{\sum_{k=2}^{\infty} \tilde{R}_k^{-1} + \sum_{l=1}^{\infty} \hat{R}_l^{-1} + \eta}, \tag{10}$$

where $=_{\mathrm{st}}$ indicates the equivalence in distribution; and $\left\{\tilde{R}_i\right\}_{i=1}^{\infty}$ $\left(\left\{\hat{R}_i\right\}_{i=1}^{\infty}\right)$ is the ascendingly ordered distances of the open (closed) BSs from the origin, obtained from a non-homogeneous 1-D Poisson point process with BS density function $\tilde{\lambda}(r)$ $\left(\hat{\lambda}(r)\right)$ defined above.

Proof: See Appendix B. ■

The next lemma shows interesting stochastic equivalences.

Lemma 2: When $\{\varepsilon_{ok}\}_{k=1}^{K} = \varepsilon_c = \varepsilon$, with respect to the HetNet SINR distribution under MIRP connectivity, the following HetNets are equivalent. All three equivalent HetNets have unity transmit power and fading factors for all tiers.

1) K open-access tiers and 1 closed-access tier with BS densities $\left\{\lambda_{ok} P_{ok}^{\frac{2}{\varepsilon}} \mathbb{E}\left[\Psi_{ok}^{\frac{2}{\varepsilon}}\right]\right\}_{k=1}^{K}$, $\lambda_c P_c^{\frac{2}{\varepsilon}} \mathbb{E}\left[\Psi_c^{\frac{2}{\varepsilon}}\right]$, respectively, and a background noise power η (same as the original HetNet).
2) 1 open-access tier and 1 closed-access tier with BS densities $\sum_{l=1}^{K} \lambda_{ol} P_{ol}^{\frac{2}{\varepsilon}} \mathbb{E}\left[\Psi_{ol}^{\frac{2}{\varepsilon}}\right]$, $\lambda_c P_c^{\frac{2}{\varepsilon}} \mathbb{E}\left[\Psi_c^{\frac{2}{\varepsilon}}\right]$, respectively, and a background noise power η.
3) 1 open-access tier and 1 closed-access tier with BS densities 1, $\hat{\lambda}_c = \frac{\lambda_c P_c^{\frac{2}{\varepsilon}} \mathbb{E}\left[\Psi_c^{\frac{2}{\varepsilon}}\right]}{\sum_{l=1}^{K} \lambda_{ol} P_{ol}^{\frac{2}{\varepsilon}} \mathbb{E}\left[\Psi_{ol}^{\frac{2}{\varepsilon}}\right]}$, respectively and a background noise power $\bar{\eta} = \eta \left(\sum_{l=1}^{K} \lambda_{ol} P_{ol}^{\frac{2}{\varepsilon}} \mathbb{E}\left[\Psi_{ol}^{\frac{2}{\varepsilon}}\right]\right)^{-\frac{\varepsilon}{2}}$.

We can express this as a function of the total number of tiers, BS densities of each open-access tier, BS density of the closed-access tier, background noise power, and the tier index of the serving BS:

$$\mathrm{SINR}_{T,I} =_{\mathrm{st}} \mathrm{SINR}\left(K+1, \left\{\lambda_{ok} P_{ok}^{\frac{2}{\varepsilon}} \mathbb{E}\left[\Psi_{ok}^{\frac{2}{\varepsilon}}\right]\right\}_{k=1}^{K}, \lambda_c P_c^{\frac{2}{\varepsilon}} \mathbb{E}\left[\Psi_c^{\frac{2}{\varepsilon}}\right], \eta, T\right) \tag{11}$$

$$=_{\mathrm{st}} \mathrm{SINR}\left(2, \sum_{l=1}^{K} \lambda_{ol} P_{ol}^{\frac{2}{\varepsilon}} \mathbb{E}\left[\Psi_{ol}^{\frac{2}{\varepsilon}}\right], \lambda_c P_c^{\frac{2}{\varepsilon}} \mathbb{E}\left[\Psi_c^{\frac{2}{\varepsilon}}\right], \eta, 1\right) \tag{12}$$

$$=_{\mathrm{st}} \mathrm{SINR}\left(2, 1, \hat{\lambda}_c, \bar{\eta}, 1\right), \tag{13}$$

where $=_{\mathrm{st}}$ indicates equivalence in distribution.

Proof: See Appendix C. ■

Lemmas 1 and 2 generalize [2, Lemma 1] and [3, Lemma 1], respectively, to the case where the HetNet also contains a closed-access tier. Next, we compute the HetNet coverage probability.

Theorem 2: The HetNet coverage probability under MIRP is

$$\mathbb{P}_{\mathrm{coverage}}^{\mathrm{MIRP}} = \sum_{k=1}^{K} \lambda_{ok} P_{ok}^{\frac{2}{\varepsilon_{ok}}} \mathbb{E}\left[\Psi_{ok}^{\frac{2}{\varepsilon_{ok}}}\right] \int_{r=0}^{\infty} 2\pi r \int_{\omega=-\infty}^{\infty} \frac{\mathrm{e}^{j\omega\eta r^{\varepsilon_{ok}}} \left(1 - \mathrm{e}^{-\frac{j\omega}{\beta_k}}\right)}{j\omega 2\pi} \mathrm{e}^{-\lambda_c P_c^{\frac{2}{\varepsilon_c}} \mathbb{E}\left[\Psi_c^{\frac{2}{\varepsilon_c}}\right] \pi r^{\frac{2\varepsilon_{ok}}{\varepsilon_c}} G\left(j\omega, \frac{2}{\varepsilon_c}\right)} \times \mathrm{e}^{-\sum_{l=1}^{K} \lambda_{ol} P_{ol}^{\frac{2}{\varepsilon_{ol}}} \mathbb{E}\left[\Psi_{ol}^{\frac{2}{\varepsilon_{ol}}}\right] \pi r^{\frac{2\varepsilon_{ok}}{\varepsilon_{ol}}} {}_1F_1\left(-\frac{2}{\varepsilon_{ol}}; 1-\frac{2}{\varepsilon_{ol}}; j\omega\right)} d\omega dr, \tag{14}$$

where $G\left(j\omega, \frac{2}{\varepsilon_c}\right) = \int_{t=0}^{\infty} \left(1 - \mathrm{e}^{j\omega t}\right) \frac{2}{\varepsilon_c} t^{-1-\frac{2}{\varepsilon_c}} dt$, and ${}_1F_1(\cdot;\cdot;\cdot)$ is called the confluent hypergeometric function of the first kind (Refer [33, Chapter 1, Section 1.7] for the definition).

Proof: The proof is along the same lines as [2, Theorem 1], and is not shown here. ■

The above expression can be greatly simplified under certain special cases, and the following results present these cases.

Corollary 4: When $\{\varepsilon_{ok}\}_{k=1}^{K} = \varepsilon_c = \varepsilon$, the HetNet coverage probability is

$$\mathbb{P}_{\mathrm{coverage}}^{\mathrm{MIRP}} = \sum_{k=1}^{K} \frac{\lambda_{ok} P_{ok}^{\frac{2}{\varepsilon}} \mathbb{E}\left[\Psi_{ok}^{\frac{2}{\varepsilon}}\right] \int_{\omega=-\infty}^{\infty} \frac{1-\mathrm{e}^{-\frac{j\omega}{\beta_k}}}{j\omega 2\pi} H(j\omega) d\omega}{\sum_{l=1}^{K} \lambda_{ol} P_{ol}^{\frac{2}{\varepsilon}} \mathbb{E}\left[\Psi_{ol}^{\frac{2}{\varepsilon}}\right]}, \tag{15}$$

$$H(j\omega) = \int_{r=0}^{\infty} 2\pi r \mathrm{e}^{j\omega\bar{\eta} r^{\varepsilon} - \pi r^2 \left({}_1F_1\left(-\frac{2}{\varepsilon}; 1-\frac{2}{\varepsilon}; j\omega\right) + \hat{\lambda}_c G\left(j\omega, \frac{2}{\varepsilon}\right)\right)} dr$$

where $H(j\omega)|_{\bar{\eta}=0} = \frac{1}{{}_1F_1\left(-\frac{2}{\varepsilon}; 1-\frac{2}{\varepsilon}; j\omega\right) + \hat{\lambda}_c G\left(j\omega, \frac{2}{\varepsilon}\right)}$, $\bar{\eta}$ and $\hat{\lambda}_c$ are from Lemma 2 and $G(\cdot,\cdot)$ is defined in Theorem 2. When $\{\beta_k\}_{k=1}^{K} = \beta$ or $\{\beta_k\}_{k=1}^{K} \geq 1$, (15) is equal to $\mathbb{P}_{\mathrm{coverage}}^{\text{max-SINR}}$. When there is no closed-access tier $\left(\hat{\lambda}_c = 0\right)$, (15) is equal to the single-tier network coverage probability (see [19, Corollary 4] and is independent of the BS transmission powers and fading factors.

Proof: The result is obtained by exchanging the order of integrations in (14) and simplifying. ■

The following theorem shows another scenario when the HetNet coverage probabilities are identical for the max-SINR and MIRP connectivity models.

Theorem 3: When $\beta_k \geq 1$, $\forall\ k = 1, \cdots, K$, the HetNet coverage probability is given by

$$\mathbb{P}_{\mathrm{coverage}}^{\text{max-SINR}} = \mathbb{P}_{\mathrm{coverage}}^{\mathrm{MIRP}} = \sum_{k=1}^{K} \frac{\lambda_{ok} P_{ok}^{\frac{2}{\varepsilon_{ok}}} \mathbb{E}\left[\Psi_{ok}^{\frac{2}{\varepsilon_{ok}}}\right] \beta_k^{-\varepsilon_k}}{\Gamma\left(1+\frac{2}{\varepsilon_{ok}}\right)} \times \int_{r=0}^{\infty} 2\pi r \times \exp\left(-\eta r^{\varepsilon_{ok}} - \frac{\lambda_c \pi P_c^{\frac{2}{\varepsilon_c}} \mathbb{E}\left[\Psi_c^{\frac{2}{\varepsilon_c}}\right] r^{\frac{2\varepsilon_{ok}}{\varepsilon_c}}}{\Gamma\left(1+\frac{2}{\varepsilon_c}\right) \mathrm{sinc}\left(\frac{2\pi}{\varepsilon_c}\right)} - \sum_{l=1}^{K} \frac{\lambda_{ol} \pi P_{ol}^{\frac{2}{\varepsilon_{ol}}} \mathbb{E}\left[\Psi_{ol}^{\frac{2}{\varepsilon_{ol}}}\right] r^{\frac{2\varepsilon_{ok}}{\varepsilon_{ol}}}}{\Gamma\left(1+\frac{2}{\varepsilon_{ol}}\right) \mathrm{sinc}\left(\frac{2\pi}{\varepsilon_{ol}}\right)}\right) dr, \tag{16}$$

and in the interference limited case ($\eta = 0$) when $\{\varepsilon_{ok}\}_{k=1}^{K} = \varepsilon_c = \varepsilon$

$$\mathbb{P}_{\text{coverage}}^{\text{maxSINR}} = \mathbb{P}_{\text{coverage}}^{\text{MIRP}} = \sum_{k=1}^{K} \frac{\lambda_{ok} P_{ok}^{\frac{2}{\varepsilon}} \mathbb{E}\left[\Psi_{ok}^{\frac{2}{\varepsilon}}\right] \operatorname{sinc}\left(\frac{2\pi}{\varepsilon}\right) \beta_k^{-\varepsilon}}{\lambda_c P_c^{\frac{2}{\varepsilon}} \mathbb{E}\left[\Psi_c^{\frac{2}{\varepsilon}}\right] + \sum_{l=1}^{K} \lambda_{ol} P_{ol}^{\frac{2}{\varepsilon}} \mathbb{E}\left[\Psi_{ol}^{\frac{2}{\varepsilon}}\right]}. \tag{17}$$

Proof: See Appendix D to derive (16), which simplifies to (17) when $\eta = 0$. ■

In the above result, (16) can be easily computed numerically and is an extension of [26, Theorem 1] to the arbitrary fading and path-loss case. Note that if there is no closed tier and $\{\beta_k\}_{k=1}^{K} = \beta$, then $\mathbb{P}_{\text{coverage}}^{\text{max-SINR}} = \mathbb{P}_{\text{coverage}}^{\text{MIRP}} = \operatorname{sinc}\left(\frac{2\pi}{\varepsilon}\right) \beta^{-\varepsilon}$. Said otherwise, if all tiers are open, there is no noise, and the pathloss exponent and threshold are the same for every tier, then adding additional tiers has no effect on performance.

The study of the MIRP connectivity has given many interesting insights and simplifications for the max-SINR case. Further, other performance metrics pertinent to HetNets such as the average fraction of load carried by each tier in the HetNet and the area-averaged rate acheived by an MS that is in coverage in a HetNet can also be derived using the results in this section. We refer the reader to [3, Theorems 2, 3 and 4] for these results. Now, we study the MBRP connectivity in further detail and its relationships to nearest-BS connectivity.

B. SINR Characterization Under MBRP Connectivity

It is clear from equations (26) and (35) that it is tedious to compute the HetNet coverage probability under nearest-BS connectivity, even with numerical integration, for the arbitrary fading case. With slight modifications to the approach in Theorem 1 and [14, Theorem 1], HetNet coverage probability with MBRP can also be derived. These expressions do not simplify significantly beyond that in (26) and hence are not presented here. Hence, we conduct a similar qualitative study of the HetNet performance under MBRP, as in Section IV-A.

Corollary 5: Under MBRP connectivity, the following stochastic equivalence holds:

$$\text{SINR}_{T,1} =_{\text{st}} \frac{\tilde{P}_{oT} \Psi_{oT1} \tilde{R}_{oT1}^{-1}}{\sum_{m=1}^{K} \sum_{l=1}^{\infty} \tilde{P}_{om} \Psi_{oml} \tilde{R}_{oml}^{-1} - \tilde{P}_{oT} \Psi_{oT1} \tilde{R}_{oT1}^{-1} + \sum_{n=1}^{\infty} \Psi_{cn} \hat{R}_{cn}^{-1} + \eta}, \tag{18}$$

where the equivalent HetNet has BS distributions according to non-homogeneous 1-D Poisson process with density functions $\left\{\tilde{\lambda}_k(r) = \lambda_{ok} \frac{2\pi}{\varepsilon_{ok}} (P_{ok} \mathbb{E}[\Psi_{ok}] B_{ok})^{\frac{2}{\varepsilon_{ok}}} r^{\frac{2}{\varepsilon_{ok}} - 1}\right\}_{k=1}^{K}$, $\hat{\lambda}(r) = \lambda_c \frac{2\pi}{\varepsilon_c} P_c^{\frac{2}{\varepsilon_c}} r^{\frac{2}{\varepsilon_c} - 1}$, $r \geq 0$, for the K open-access tiers and the closed-access tier, respectively, transmission power of the m^{th} $(m = 1, \ldots, K)$ open-access tier BSs are $\tilde{P}_{om} = (\mathbb{E}[\Psi_{om}] B_{om})^{-1}$ and unity for the closed-access tier BSs; and unity path-loss exponent for all BSs, but the fading factor distributions are the same as the original HetNet.

Proof: From (8), $T = \underset{m=1,\cdots,K}{\arg\max} P_{om} R_{om1}^{-\varepsilon_{om}} \mathbb{E}[\Psi_{om}] B_{om}$

$$\mathbb{P}\left(\{\text{SINR}_{T,1} > \beta_T\}\right) = \mathbb{P}\left(\left\{\frac{P_{oT} \Psi_{oT1} R_{oT1}^{-\varepsilon_{oT}}}{I_o - P_{oT} \Psi_{oT1} R_{oT1}^{-\varepsilon_{oT}} + I_c + \eta} > \beta_T\right\}\right),$$

where I_o and I_c are defined in (1). Now, as in the proof of Lemma 1, using [2, Theorem 2], let us consider the set $\left\{\tilde{R}_{omi} = (P_{om} \mathbb{E}[\Psi_{om}] B_{om})^{-1} R_{omi}^{\varepsilon_{om}}\right\}_{i=1}^{\infty}$ as a set of distances from the origin of m^{th} tier BSs from the origin in an equivalent HetNet. Using the Marking theorem of Poisson processes [32, Page 55], the equivalent HetNet is from a non-homogeneous Poisson point process with a BS density function $\tilde{\lambda}_{om}(r)$, $r \geq 0$, $\forall\, m = 1, \cdots, K$ as shown in Corollary 5. Further, the serving BS is the closest among all the open-access BSs of the HetNet. Finally, the m^{th} tier transmit power of the equivalent system, $\tilde{P}_{om}$, is obtained to ensure that the received power at the MS is stochastically equivalent to that of the original cellular system. ■

The result is yet another application of the Marking theorem of Poisson processes, and can be proved using the same techniques as developed in Lemma 1. The next result characterizes the serving BS under the MBRP case.

Lemma 3: For the serving BS under MBRP connectivity, the probability mass function (p.m.f.) of its tier-index and the joint p.d.f. of its tier-index and distance from the MS are

$$\mathbb{P}(\{T = k\}) = \int_{r=0}^{\infty} \tilde{\lambda}_{ok}(r) \cdot \mathrm{e}^{-\sum_{l=1}^{K} \lambda_{ol} \pi (P_{ol} \mathbb{E}[\Psi_{ol}] B_{ol})^{\frac{2}{\varepsilon_{ol}}} r^{\frac{2}{\varepsilon_{ol}}}} dr, \tag{19}$$

$$f_{T, \tilde{R}_{oT,1}}(k, r) = \tilde{\lambda}_{ok}(r) \cdot \mathrm{e}^{-\sum_{l=1}^{K} \lambda_{ol} \pi (P_{ol} \mathbb{E}[\Psi_{ol}] B_{ol})^{\frac{2}{\varepsilon_{ol}}} r^{\frac{2}{\varepsilon_{ol}}}}, \tag{20}$$

for $k = 1, \cdots, K$, where $\tilde{\lambda}_{ok}(r)$and $\tilde{R}_{oT,1}$ are from Corollary 5. When $\{\varepsilon_{ol}\}_{l=1}^{K} = \varepsilon$,

$$\mathbb{P}(\{T = k\}) = \frac{\lambda_{ok} (P_{ok} \mathbb{E}[\Psi_{ok}] B_{ok})^{\frac{2}{\varepsilon}}}{\sum_{l=1}^{K} \lambda_{ol} (P_{ol} \mathbb{E}[\Psi_{ol}] B_{ol})^{\frac{2}{\varepsilon}}}. \tag{21}$$

Proof: Along the same lines as [2, Lemmas 3 and 4], the c.c.d.f. of the distance of the serving BS belonging to the k^{th} open-access tier are derived.

$$\begin{aligned}
&\mathbb{P}\left(\{T = k\} \bigcap \left\{\tilde{R}_{ok1} > r\right\}\right) \overset{(a)}{=} \\
&\mathbb{P}\left(\bigcap_{l=1,\, l \neq k}^{K} \left\{\tilde{R}_{ol1} > \tilde{R}_{ok1}\right\} \bigcap \left\{\tilde{R}_{ok1} > r\right\}\right) = \\
&\mathbb{E}_{\tilde{R}_{ok1}}\left[\mathbb{I}\left(\tilde{R}_{ok1} > r\right) \mathbb{P}\left(\bigcap_{l=1,\, l \neq k}^{K} \left\{\tilde{R}_{ol1} > \tilde{R}_{ok1}\right\} \middle| \tilde{R}_{ok1}\right)\right] \\
&\overset{(b)}{=} \int_{t=r}^{\infty} \tilde{\lambda}_{ok}(t) \, \mathrm{e}^{-\sum_{l=1}^{K} \int_{s=0}^{t} \tilde{\lambda}_{ol}(s) ds} dt,
\end{aligned} \tag{22}$$

where (a) is obtained since the serving BS belongs to the k^{th} tier if the nearest BS among all the open-access tiers in the equivalent HetNet of Corollary 5 belongs to the k^{th} tier and

(b) is obtained by noting that $\left\{\tilde{R}_{ol1}\right\}_{l=1}^{K}$ is a set of independent random variables with the p.d.f. of $\tilde{R}_{ol1}$ as $f_{\tilde{R}_{ol1}}(r) = \tilde{\lambda}_{ol}(r) \cdot \mathrm{e}^{-\int_{s=0}^{r} \tilde{\lambda}_{ol}(s)ds}$, $r \geq 0$ from the properties of Poisson process. Computing the integrals and setting $r = 0$ yields (19), while taking the derivative with respect to r yields (20). ■

When $\{\mathbb{E}[\Psi_{ol}]\}_{l=1}^{K} = 1$, (19) and (21) reduce to [30, (3) and (4)], respectively. Deriving the coverage probability expressions for the arbitrary fading distribution case under MBRP suffers from similar analytical intractabilities as the nearest-BS case studied in Section III. Hence, we consider the special case where fading factors are i.i.d. unit mean exponential random variables. In [30], Jo et. al. have demonstrated that simple expressions for the HetNet coverage probability under MARP can be computed when the fading factors are i.i.d. exponential random variables. These results were restricted to the open-access case. We extend to a general HetNet below.

Theorem 4: The HetNet coverage probability under MBRP connectivity with i.i.d. exponentially distributed fading factors at all BSs is

$$\mathbb{P}_{\text{coverage}}^{\text{MBRP}} = \sum_{k=1}^{K} \lambda_{ok} P_{ok}^{\frac{2}{\varepsilon_{ok}}} \beta_k^{-\frac{2}{\varepsilon_{ok}}} \int_{r=0}^{\infty} 2\pi r \mathrm{e}^{-\eta r^{\varepsilon_{ok}}} \times \mathrm{e}^{-\frac{\lambda_c \pi P_c^{\frac{2}{\varepsilon_c}} r^{\frac{2\varepsilon_{ok}}{\varepsilon_c}}}{\mathrm{sinc}\left(\frac{2\pi}{\varepsilon_c}\right)} - \sum_{l=1}^{K} \lambda_{ol} \pi P_{ol}^{\frac{2}{\varepsilon_{ol}}} F(\beta_k, \varepsilon_{ol}) r^{\frac{2\varepsilon_{ok}}{\varepsilon_{ol}}}} dr \quad (23)$$

where $F(\beta_k, \varepsilon_{ol}) = \beta_k^{-\frac{2}{\varepsilon_{ol}}} \left[1 - {}_2F_1\left(1, \frac{2}{\varepsilon_{ol}}; 1 + \frac{2}{\varepsilon_{ol}}; -\beta_k^{-1}\right)\right] + \frac{1}{\mathrm{sinc}\left(\frac{2\pi}{\varepsilon_{ol}}\right)}$. When $\{\varepsilon_{ok}\}_{k=1}^{K} = \varepsilon$ and $\eta = 0$,

$$\mathbb{P}_{\text{coverage}}^{\text{nearest}} = \mathbb{P}_{\text{coverage}}^{\text{MARP}} = \sum_{k=1}^{K} \frac{\lambda_{ok} P_{ok}^{\frac{2}{\varepsilon}} \beta_k^{-\frac{2}{\varepsilon}} \mathrm{sinc}\left(\frac{2\pi}{\varepsilon}\right)}{\lambda_c P_c^{\frac{2}{\varepsilon}} + \sum_{l=1}^{K} \lambda_{ol} P_{ol}^{\frac{2}{\varepsilon}} F(\beta_k, \varepsilon) \mathrm{sinc}\left(\frac{2\pi}{\varepsilon}\right)}. \quad (24)$$

Proof: See Appendix E. ■

The above is a generalization of [30, Theorem 1] to the closed-access case. Further, comparing (17) and (24), clearly, $\mathbb{P}_{\text{coverage}}^{\text{MIRP}} \geq \mathbb{P}_{\text{coverage}}^{\text{MARP}}$, when $\{\beta_k\}_{k=1}^{\infty} \geq 1$ since $F(\beta_k, \varepsilon_{ol}) \mathrm{sinc}\left(\frac{2\pi}{\varepsilon_{ol}}\right) \geq 1, \forall\, \beta_k \geq 0, \varepsilon_{ol} > 2$.

V. Numerical Examples and Discussion

In this section, we provide some numerical examples that complement the theoretical results presented until now. We restrict ourselves to the study of a two tier HetNet consisting of the macrocell and the femtocell networks, under the max-SINR connectivity model. More tiers and other models can be analyzed but this is suggestive of the kinds of results we can derive. It is also representative because we have shown in many cases the analysis of many tiers can be reduced to analyzing one or a few tiers. Please refer to Appendix F for the algorithm to perform the Monte-Carlo simulations. The simulation results in the graphs are the lines and the semi-analytic results are the marks. These lie on top of each other for all of the graphs. For all the studies in this paper, $\lambda_2 = 5\lambda_1$, $P_1 = 25P_2$, $\varepsilon = 3$, $\beta_2 = 1$ dB, and η =0 where the subscripts '1' and '2' correspond to macrocell and femtocell networks, respectively. Further, under the closed-access BS association scheme, the MS has access to the macrocell network only.

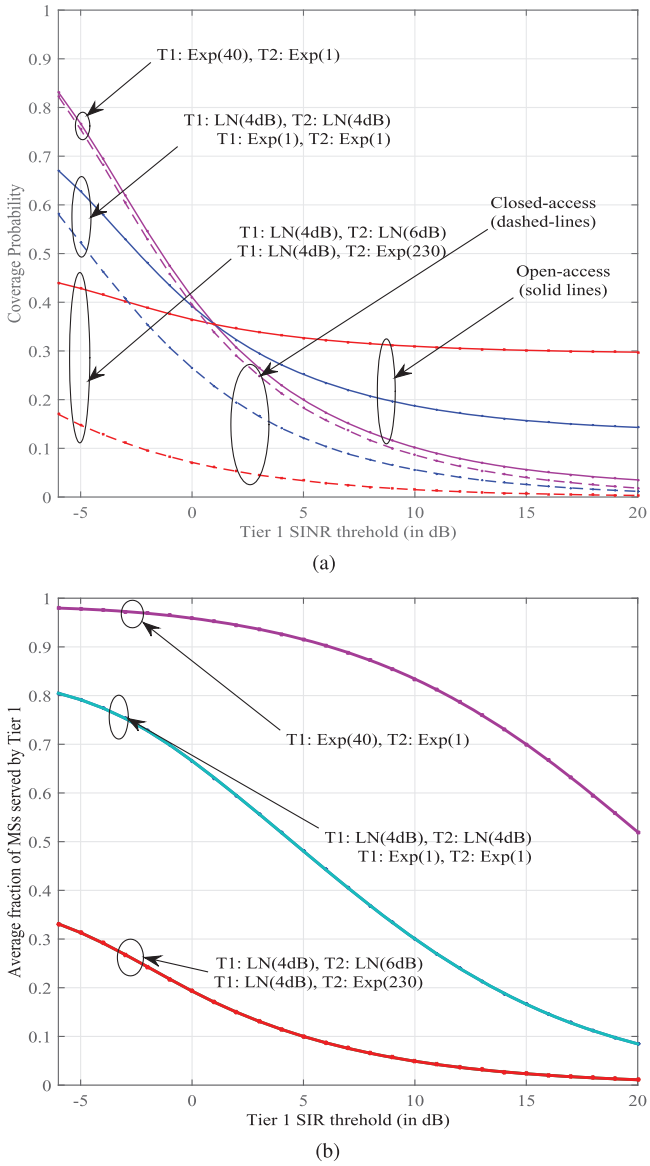

Fig. 1. Two-tier HetNet (a) Comparing coverage probabilities for various fading distributions, (b) Average fraction of MSs served by macrocell BSs vs macrocell SIR threshold.

In Figures 1a, 1b and 2, we study the coverage probability, the average fraction of users served by the macrocell network, and coverage conditional average rate for various configurations of fading distributions at the macrocell and the femtocell BSs. Note that the expressions for the coverage conditional average rate and the average fraction of users served by the macrocell network can be found in [3, Theorems 2, 3 and 4] and are included to show the applicability of the results. In all the figures, T1 and T2 stand for tier 1 and tier 2. Further, the fading factor distributions are either exponential (Exp(·)) with a given mean or log normal (LN(·)) with a zero mean and given

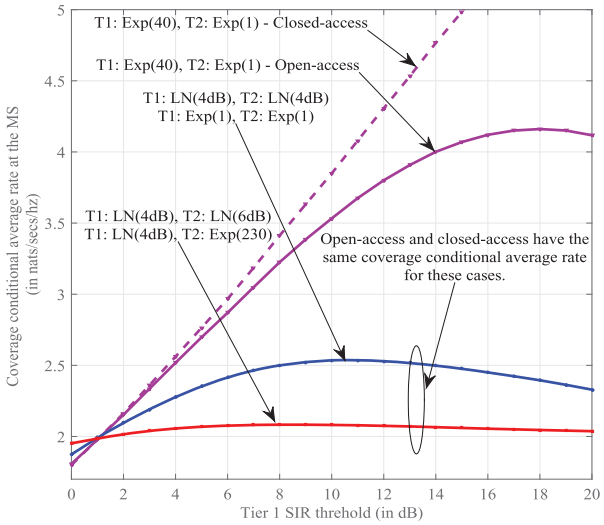

Fig. 2. Two-tier HetNet: Variation of coverage conditional average rate with Tier 1 SIR threshold and different fading distributions.

standard deviation (when the random variable is expressed in dB).

The plots in Figure 1a clearly show that a MS has a better coverage probability under open-access than closed-access as predicted by Theorem 3. The top plot (T1: Exp(40), T2: Exp(1)) is equivalent to the case where $P_1 = 1000P_2$, with the fading factors at both the tiers being unit mean exponential distributions. The open and closed access have approximately the same coverage probabilities because the MS is almost always served by a macrocell BS, as can been seen in the corresponding curve in Figure 1b. As a result, blocking access to the femtocell BSs altogether, has only a marginal influence on the coverage probability at the MS.

When both tiers have the same fading factor distribution, the coverage probability becomes independent of the exact distribution as shown in (15). This is shown by the next two curves (T1: LN(4dB), T2: LN(4dB)) and (T1: Exp(1), and T2: Exp(1)) in the figures which each have this characteristic and lie on top of each other. We also note in (15) that the only component of the fading factor that is important is $\mathbb{E}\left[\Psi^{\frac{2}{\varepsilon}}\right]$. This is shown in the last two curves (T1: LN(4dB), T2: LN(6dB)) and (T1: LN(4dB), T2: Exp(230)) which lie on top of each other since LN(6dB) and Exp(230) have the same $(2/\varepsilon)^{\text{th}}$ moments.

Under open-access, the coverage probability and the coverage conditional average rate (see Figures 1a and 2) for all the 5 curves mentioned above intersect when the SIR threshold for the macrocell network is equal to 1 dB. This brings us to an important point. Given all open tiers and no noise, when the SIR threshold and path loss exponent is the same for all the tiers, these become the only factors that affect the performance and all fading factors, transmit power, and BS density drop out.

VI. Conclusions

In this paper, for the most general model of the HetNets, the downlink coverage probability and other related performance metrics such as the average downlink rate and average fraction of users served by each tier of the HetNet are characterized. Two important BS connectivity models are studied, namely, the max-SINR and the nearest-BS connectivity, respectively. Semi-analytical expressions for the HetNet coverage probability is obtained for both the cases. Further, several properties pertaining to the HetNet downlink performance are analyzed, which provide great insights about these complex networks. As an example, we identify the MIRP and MBRP connectivity models to be equivalent to the former models under certain special conditions. These models are much simpler to analyze and the results for these models expose interesting properties of the HetNet. The results admit arbitrarily distributed fading factors. So, they can be applied to scenarios that consider either fast or slow fading or a combined fading. The results in this paper greatly generalize the existing HetNet performance characterization results and are essential for better understanding of the future developments in wireless communications that are heavily based on HetNets. Future work will address fast and slow fading when treated separately.

Appendix

A. Proof for Theorem 1

The coverage probability expressions in (2) and (3) can be equivalently expressed as follows:

$$\mathbb{P}_{\text{coverage}}^{\text{max-SINR}} = \mathbb{P}\left(\bigcup_{k=1}^{K}\left\{\frac{M_k}{I_o + I_c + \eta - M_k} > \beta_k\right\}\right) = \mathbb{P}\left(\left\{\max_{k=1,\cdots,K} \gamma_k M_k > I_o + I_c + \eta\right\}\right), \quad (25)$$

$$\mathbb{P}_{\text{coverage}}^{\text{nearest}} = \mathbb{P}\left(\bigcup_{k=1}^{K}\left\{\frac{N_k}{I_o + I_c + \eta - N_k} > \beta_k\right\}\right) = \mathbb{P}\left(\left\{\max_{k=1,\cdots,K} \gamma_k N_k > I_o + I_c + \eta\right\}\right), \quad (26)$$

where β_k, γ_k are defined in Table I, $M_k = \max_{l=1,\cdots,\infty} P_{ok}\Psi_{okl}R_{okl}^{-\varepsilon_{ok}}$ is the maximum of the received powers from all the k^{th} tier's BSs, $N_k = P_{ok}\Psi_{ok1}R_{ok1}^{-\varepsilon_{ok}}$ is the received power from the nearest BS among all the k^{th} tier's BSs, $I_o + I_c + \eta$ is the total received power at the MS, η is the background noise power, and I_o, I_c (defined in (1)) are the sum of the received powers from all the open-access BSs and closed-access BSs in the system, respectively. Notice from (25) and (26) that the HetNet coverage probability can be obtained if the joint probability density function (p.d.f.) of $\left(I_o + I_c + \eta, \max_{i=1,\cdots,K} \gamma_i M_i\right)$ and $\left(I_o + I_c + \eta, \max_{i=1,\cdots,K} \gamma_i N_i\right)$ is known, respectively. Using

the same steps as in the proof of [14, Corollary 4], the above mentioned joint p.d.f.s can be expressed as

$$f_{I_o+I_c+\eta,\ \max\limits_{i=1,\cdots,K}\gamma_i M_i}(x,y) = \int_{\omega=-\infty}^{\infty} \frac{\partial}{\partial u}\mathcal{L}_{I_o+I_c+\eta,\ \max\limits_{i=1,\cdots,K}\gamma_i M_i\le u}(j\omega)\Big|_{u=y} \frac{\mathrm{e}^{j\omega x}}{2\pi}d\omega, \quad (27)$$

$$f_{I_o+I_c+\eta,\ \max\limits_{i=1,\cdots,K}\gamma_i N_i}(x,y) = \int_{\omega=-\infty}^{\infty} \frac{\partial}{\partial u}\mathcal{L}_{I_o+I_c+\eta,\ \max\limits_{i=1,\cdots,K}\gamma_i N_i\le u}(j\omega)\Big|_{u=y} \frac{\mathrm{e}^{j\omega x}}{2\pi}d\omega, \quad (28)$$

where $f_{.,.}(\cdot,\cdot)$ denotes the joint p.d.f. of the involved random variables:

$$\mathcal{L}_{I_o+I_c+\eta,\ \max\limits_{k=1,\cdots,K}\gamma_k M_k\le u}(s) \triangleq \mathbb{E}\left[\mathrm{e}^{-s(I_o+I_c+\eta)}\mathcal{I}\left(\max_{k=1,\cdots,K}\gamma_k M_k \le u\right)\right],$$

$$\mathcal{L}_{I_o+I_c+\eta,\ \max\limits_{k=1,\cdots,K}\gamma_k N_k\le u}(s) \triangleq \mathbb{E}\left[\mathrm{e}^{-s(I_o+I_c+\eta)}\mathcal{I}\left(\max_{k=1,\cdots,K}\gamma_k N_k \le u\right)\right]$$

denote the Laplace transform function of the total received power at the MS $(I_o + I_c + \eta)$ such that the received power from the desired serving BS of each open-access tier satisfies the constraint $\gamma_k M_k \le u$ and $\gamma_k N_k \le u$, for the max-SINR connectivity and the nearest BS connnectivity models, respectively; and $\mathcal{I}(\cdot)$ is the indicator function. In order to avoid repetition, we refer the reader to [14, Corollary 4] for the intermediate steps for the derivation of (27) and (28). We begin with computing the Laplace transform of the interference from the closed-access tiers, I_c, $\mathcal{L}_{I_c}(s) = \mathbb{E}\left[\mathrm{e}^{-sI_c}\right]$.

Lemma 4: The Laplace transform of the interference from the closed-access tiers is

$$\mathcal{L}_{I_c}(s) = \mathrm{e}^{-\sum_{l=1}^{L}\lambda_{cl}\pi(sP_{cl})^{\frac{2}{\varepsilon_{cl}}}\mathbb{E}\left[\Psi_{cl}^{\frac{2}{\varepsilon_{cl}}}\right]\Gamma\left(1-\frac{2}{\varepsilon_{cl}}\right)}. \quad (29)$$

Proof: The proof for (29) is as follows.

$$\mathcal{L}_{I_c}(s) = \mathbb{E}\left[\exp\left(-s\sum_{l=1}^{L}\sum_{n=1}^{\infty}P_{cl}\Psi_{cln}R_{cln}^{-\varepsilon_{cl}}\right)\right] \overset{(a)}{=} \prod_{l=1}^{L}\mathbb{E}\left[\exp\left(-s\sum_{n=1}^{\infty}P_{cl}\Psi_{cln}R_{cln}^{-\varepsilon_{cl}}\right)\right] \overset{(b)}{=} \prod_{l=1}^{L}\exp\left(-\lambda_{cl}\mathbb{E}_{\Psi_{cl}}\left[\int_{r=0}^{\infty}\left(1-\mathrm{e}^{-sP_{cl}\Psi_{cl}r^{-\varepsilon_{cl}}}\right)2\pi r dr\right]\right),$$

where (a) is obtained because the BS arrangement for the L closed-access tiers and the corresponding transmission and fading factors are independent of each other, and (b) evaluates the expectation in (a) using Campbell's theorem for a Poisson point process [32, Page 28], and (29) is obtained by evaluating the integral in the expression of the equality (b). ■

Next, we derive expressions for the two Laplace tranform functions in (27) and (28) that will later be used to obtain semi-analytical expressions for $\mathbb{P}_{\text{coverage}}^{\text{max-SINR}}$ and $\mathbb{P}_{\text{coverage}}^{\text{nearest}}$, respectively.

Lemma 5:

$$\mathcal{L}_{I_o+I_c+\eta,\ \max\limits_{k=1,\cdots,K}\gamma_k M_k\le u}(s) = \mathcal{L}_{I_c}(s)\times \exp\left(-s\eta-\sum_{k=1}^{K}\lambda_{ok}\pi\,(sP_{ok})^{\frac{2}{\varepsilon_{ok}}}\,\mathbb{E}\left[\Psi_{ok}^{\frac{2}{\varepsilon_{ok}}}\right]\times\left[\Gamma\left(1-\frac{2}{\varepsilon_{ok}}\right)+\frac{2}{\varepsilon_{ok}}\Gamma\left(-\frac{2}{\varepsilon_{ok}},\frac{su}{\gamma_k}\right)\right]\right), \quad (30)$$

$$\mathcal{L}_{I_o+I_c+\eta,\ \max\limits_{k=1,\cdots,K}\gamma_k N_k\le u}(s) = \mathcal{L}_{I_c}(s)\,\mathrm{e}^{-s\eta-\sum_{k=1}^{K}\lambda_{ok}\pi(sP_{ok})^{\frac{2}{\varepsilon_{ok}}}\mathbb{E}\left[\Psi_{ok}^{\frac{2}{\varepsilon_{ok}}}\right]\Gamma\left(1-\frac{2}{\varepsilon_{ok}}\right)}\times \prod_{k=1}^{K}\mathbb{E}_{\Psi_{ok1}}\left[\int_{x=0}^{\frac{su}{\gamma_k\Psi_{ok1}}}\lambda_{ok}\frac{2\pi}{\varepsilon_{ok}}(sP_{ok})^{\frac{2}{\varepsilon_{ok}}}x^{-\frac{2}{\varepsilon_{ok}}-1}\times \mathrm{e}^{-\Psi_{ok1}x-\lambda_{ok}\frac{2\pi}{\varepsilon_{ok}}(sP_{ok})^{\frac{2}{\varepsilon_{ok}}}\mathbb{E}_{\Psi_{ok}}\left[\Psi_{ok}^{\frac{2}{\varepsilon_{ok}}}\Gamma\left(-\frac{2}{\varepsilon_{ok}},x\Psi_{ok}\right)\right]}dx\right], \quad (31)$$

where $u \ge 0$, $\mathcal{L}_{I_c}(s)$ is from Lemma 4 and the random variables Ψ_{ok1} and Ψ_{ok} are i.i.d. for all $k = 1, \cdots, K$.

Proof: The proof for (30) is shown below.

$$\mathcal{L}_{I_o+I_c+\eta,\ \max\limits_{k=1,\cdots,K}\gamma_k M_k\le u}(s) = \mathbb{E}\left[\exp\left(-s\left(I_o+I_c+\eta\right)\right)\times\mathcal{I}\left(\max_{k=1,\cdots,K}\gamma_k M_k\le u\right)\right] \overset{(a)}{=} \mathcal{L}_{I_c}(s)\,\mathrm{e}^{-s\eta}\times \mathbb{E}\left[\prod_{k=1}^{K}\prod_{l=1}^{\infty}\mathrm{e}^{-sP_{ok}\Psi_{okl}R_{okl}^{-\varepsilon_{ok}}}\mathcal{I}\left(\gamma_k P_{ok}\Psi_{okl}R_{okl}^{-\varepsilon_{ok}}\le u\right)\right] \overset{(b)}{=} \mathcal{L}_{I_c}(s)\,\mathrm{e}^{-s\eta}\times \prod_{k=1}^{K}\mathbb{E}\left[\prod_{l=1}^{\infty}\mathrm{e}^{-sP_{ok}\Psi_{okl}R_{okl}^{-\varepsilon_{ok}}}\mathcal{I}\left(P_{ok}\Psi_{okl}R_{okl}^{-\varepsilon_{ok}}\le\frac{u}{\gamma_k}\right)\right]$$

$$\overset{(c)}{=} \mathcal{L}_{I_c}(s)\,\mathrm{e}^{-s\eta}\prod_{k=1}^{K}\exp\left(-\lambda_{ok}\int_{r=0}^{\infty}\left(1-\mathbb{E}\left[\mathrm{e}^{-sP_{ok}\Psi_{ok}r^{-\varepsilon_{ok}}}\mathcal{I}\left(P_{ok}\Psi_{ok}r^{-\varepsilon_{ok}}\le\frac{u}{\gamma_k}\right)\right]\right)2\pi r dr\right)$$

$$\overset{(d)}{=} \mathcal{L}_{I_c}(s)\,\mathrm{e}^{-s\eta}\prod_{k=1}^{K}\exp\left(-\lambda_{ok}\mathbb{E}_{\Psi_{ok}}\left[\int_{t=0}^{\infty}\left(1-\mathrm{e}^{-t}\mathcal{I}\left(t\le\frac{su}{\gamma_k}\right)\right)\frac{2\pi}{\varepsilon_{ok}}t^{-\frac{2}{\varepsilon_{ok}}-1}(sP_{ok}\Psi_{ok})^{\frac{2}{\varepsilon_{ok}}}dt\right]\right)$$

$$\overset{(e)}{=} \mathcal{L}_{I_c}(s)\,\mathrm{e}^{-s\eta}\prod_{k=1}^{K}\exp\left(-\lambda_{ok}\pi\,(sP_{ok})^{\frac{2}{\varepsilon_{ok}}}\,\mathbb{E}\left[\Psi_{ok}^{\frac{2}{\varepsilon_{ok}}}\right]\times\left[\Gamma\left(1-\frac{2}{\varepsilon_{ok}}\right)+\frac{2}{\varepsilon_{ok}}\int_{t=0}^{\infty}\mathrm{e}^{-t}t^{-\frac{2}{\varepsilon_{ok}}-1}\mathcal{I}\left(t>\frac{su}{\gamma_k}\right)dt\right]\right) \quad (32)$$

where (a) is obtained by noting that I_c is independent of the random variables I_o and $\max\limits_{k=1,\cdots,K}\gamma_k M_k \le u$, $\mathcal{L}_{I_c}(s)$ is a

direct consequence of Campbell's theorem [32], $\mathrm{e}^{-s\eta}$ is a constant and $\left\{\max_{k=1,\cdots,K}\gamma_k M_k \le u\right\} \iff \left\{\gamma_k P_{ok}\Psi_{okl}R_{okl}^{-\varepsilon_{ok}} \le u\right\}$, $\forall\ k=1,\cdots,\ K$ and $l=1,\ 2,\cdots$; (b) is obtained since the random variables corresponding to a given tier are independent of the other tiers; (c) is obtained by applying Campbell's theorem [32] to each tier of the HetNet; (d) is obtained by changing the variable of integration from r to $t = sP_{ok}\Psi_{ok}r^{-\varepsilon_{ok}}$; (e) is obtained by rewriting the integral in (d) using special functions; and finally (30) is obtained by rewriting the integral in (e) in terms of the incomplete Gamma function.

The proof for (31) follows along the same lines as above and we provide a brief outline below:

$$
\begin{aligned}
&\frac{\mathcal{L}_{I_o+I_c+\eta,\ \max_{k=1,\cdots,K}\gamma_k N_k\le u}(s)}{\mathcal{L}_{I_c}(s)\,\mathrm{e}^{-s\eta}}\\
&\overset{(a)}{=}\mathbb{E}\left[\prod_{k=1}^{K}\prod_{l=1}^{\infty}\mathrm{e}^{-sP_{ok}\Psi_{okl}R_{okl}^{-\varepsilon_{ok}}}\mathcal{I}\left(\max_{k=1,\cdots,K}\frac{\gamma_k P_{ok}\Psi_{ok1}}{R_{ok1}^{\varepsilon_{ok}}}\le u\right)\right]\\
&=\mathbb{E}\left[\prod_{k=1}^{K}\prod_{l=1}^{\infty}\mathrm{e}^{-sP_{ok}\Psi_{okl}R_{okl}^{-\varepsilon_{ok}}+\ln\left(\mathcal{I}\left(\gamma_k P_{ok}\Psi_{ok1}R_{ok1}^{-\varepsilon_{ok}}\le u\right)\right)}\right]\\
&\overset{(b)}{=}\prod_{k=1}^{K}\mathbb{E}_{\Psi_{ok1},R_{ok1}}\left[\mathrm{e}^{-sP_{ok}\Psi_{ok1}R_{ok1}^{-\varepsilon_{ok}}}\mathcal{I}\left(\gamma_k P_{ok}\Psi_{ok1}R_{ok1}^{-\varepsilon_{ok}}\le u\right)\right.\\
&\left.\times\mathbb{E}\left[\prod_{l=2}^{\infty}\mathrm{e}^{-sP_{ok}\Psi_{okl}R_{okl}^{-\varepsilon_{ok}}\mathcal{I}(R_{okl}>R_{ok1})}\,\middle|\,R_{ok1}\right]\right]\\
&\overset{(c)}{=}\prod_{k=1}^{K}\mathbb{E}_{\Psi_{ok1},R_{ok1}}\left[\mathrm{e}^{-sP_{ok}\Psi_{ok1}R_{ok1}^{-\varepsilon_{ok}}}\mathcal{I}\left(\gamma_k P_{ok}\Psi_{ok1}R_{ok1}^{-\varepsilon_{ok}}\le u\right)\right.\\
&\left.\times\mathrm{e}^{-\lambda_{ok}\int_{r=R_{ok1}}^{\infty}\left(1-\mathbb{E}\left[\mathrm{e}^{-sP_{ok}\Psi_{ok}r^{-\varepsilon_{ok}}}\right]\right)2\pi r dr}\right]\\
&\overset{(d)}{=}\prod_{k=1}^{K}\mathbb{E}_{\Psi_{ok1},R_{ok1}}\left[\mathrm{e}^{-sP_{ok}\Psi_{ok1}R_{ok1}^{-\varepsilon_{ok}}}\mathcal{I}\left(\gamma_k P_{ok}\Psi_{ok1}R_{ok1}^{-\varepsilon_{ok}}\le u\right)\right.\\
&\left.\times\exp\left(-\lambda_{ok}\pi\,(sP_{ok})^{\frac{2}{\varepsilon_{ok}}}\times\right.\right.\\
&\left.\left.\mathbb{E}_{\Psi_{ok}}\left[\Psi_{ok}^{\frac{2}{\varepsilon_{ok}}}\int_{t=0}^{sP_{ok}\Psi_{ok}R_{ok1}^{-\varepsilon_{ok}}}\left(1-\mathrm{e}^{-t}\right)\frac{2}{\varepsilon_{ok}}t^{-\frac{2}{\varepsilon_{ok}}-1}dt\right]\right)\right]
\end{aligned}
\tag{33}
$$

where the maximization in (a) is only among the nearest BSs of the K tiers of the HetNet, $\mathcal{L}_{I_c}(s)$ is defined in (32); (b) is obtained by exchanging the order of expectation and product since the K tiers of the HetNet are independent of each other, and further conditioning w.r.t. the fading factors and the distance of the nearest BS of each tier; (c) is obtained by applying Campbell's theorem to the set of k^{th} tier BSs beyond R_{ok1}, conditioned on R_{ok1}; (d) is obtained by further simplifying (c); and finally (31) is obtained by evaluating the expectation w.r.t. R_{ok1} in (d) where the p.d.f. of R_{ok1} is $f_{R_{ok1}}(r) = \lambda_{ok}2\pi r\mathrm{e}^{-\lambda_{ok}\pi r^2},\ r\ge 0$, and further simplifying. ■

Next, the partial derivative of the Laplace transform function in (30) and (31) w.r.t. u are shown, which are in turn used to compute the joint p.d.f.s of $\left(I_o+I_c+\eta,\ \max_{i=1,\cdots,K}\gamma_i M_i\right)$ and $\left(I_o+I_c+\eta,\ \max_{i=1,\cdots,K}\gamma_i N_i\right)$ shown in (27) and (28), respectively. We leave the proof to the interested readers as it involves straightforward algebraic manipulation after taking the partial derivative w.r.t. u to obtain (34) and (35), shown at the bottom of the page.

To compare this result with [27], we note that for a unit mean exponential random variable $\mathbb{E}\left[\Psi_{ok}^{\frac{2}{\varepsilon_{ok}}}\right] = \Gamma\left(1+\frac{2}{\varepsilon_{ok}}\right)$. Setting $\{\lambda_{cl}\}_{l=1}^{L}=0$ and $\{\varepsilon_{ok}\}_{k=1}^{K}=\alpha$, (34) reduces to [27, (2)]. Having computed the expressions for the joint p.d.f.'s in (27) and (28), the coverage probabilities equations derived in Theorem 1 can be proved below.

Once the joint p.d.f. has been obtained (see (27) and (28)), the probability of the event in (25) can be derived as follows:

$$
\begin{aligned}
\mathbb{P}_{\text{coverage}}^{\text{max-SINR}} &\overset{(a)}{=}\mathbb{P}\left(\left\{\frac{1}{\kappa}\max_{i=1,\cdots,K}\gamma_i M_i+\eta<\right.\right.\\
&\left.\left.I_o+I_c+\eta<\max_{i=1,\cdots,K}\gamma_i M_i\right\}\right)\\
&\overset{(b)}{=}\int_{y=0}^{\infty}\int_{x=\frac{y}{\kappa}+\eta}^{y} f_{I_o+I_c+\eta,\ \max_{i=1,\cdots,K}\gamma_i M_i}(x,y)\,dxdy\\
&\overset{(c)}{=}\int_{y=0}^{\infty}\int_{\omega=-\infty}^{\infty}\frac{\partial}{\partial u}\mathcal{L}_{I_o+I_c+\eta,\ \max_{i=1,\cdots,K}\gamma_i M_i\le y}(j\omega)\Big|_{u=y}\\
&\times\frac{\mathrm{e}^{j\omega y}-\mathrm{e}^{j\omega\left(\frac{y}{\kappa}+\eta\right)}}{j\omega 2\pi}d\omega dy,
\end{aligned}
$$

$$
\frac{\frac{\partial}{\partial u}\mathcal{L}_{I_o+I_c+\eta,\ \max_{i=1,\cdots,K}\gamma_i M_i\le u}(s)}{\mathcal{L}_{I_o+I_c+\eta,\ \max_{i=1,\cdots,K}\gamma_i M_i\le u}(s)} = \sum_{k=1}^{K}\lambda_{ok}\frac{2\pi}{\varepsilon_{ok}}(\gamma_k P_{ok})^{\frac{2}{\varepsilon_{ok}}}\,\mathbb{E}\left[\Psi_{ok}^{\frac{2}{\varepsilon_{ok}}}\right]u^{-1-\frac{2}{\varepsilon_{ok}}}\mathrm{e}^{-\frac{su}{\gamma_k}}, \tag{34}
$$

$$
\frac{\frac{\partial}{\partial u}\mathcal{L}_{I_o+I_c+\eta,\ \max_{i=1,\cdots,K}\gamma_i N_i\le u}(s)}{\mathcal{L}_{I_o+I_c+\eta,\ \max_{i=1,\cdots,K}\gamma_i N_i\le u}(s)} = \sum_{k=1}^{K}\frac{\frac{\mathbb{E}_{\Psi_{ok1}}\left[\Psi_{ok1}^{\frac{2}{\varepsilon_{ok}}}\mathrm{e}^{-\lambda_{ok}\frac{2\pi}{\varepsilon_{ok}}(sP_{ok})^{\frac{2}{\varepsilon_{ok}}}\mathbb{E}_{\Psi_{ok}}\left[\Psi_{ok}^{\frac{2}{\varepsilon_{ok}}}\Gamma\left(-\frac{2}{\varepsilon_{ok}},\frac{su\Psi_{ok}}{\gamma_k\Psi_{ok1}}\right)\right]}\right]}{u\mathrm{e}^{\frac{su}{\gamma_k}}}}{\int_{x=0}^{1}\frac{\mathbb{E}_{\Psi_{ok1}}\left[\Psi_{ok1}^{\frac{2}{\varepsilon_{ok}}}\mathrm{e}^{-\lambda_{ok}\frac{2\pi}{\varepsilon_{ok}}(sP_{ok})^{\frac{2}{\varepsilon_{ok}}}\mathbb{E}_{\Psi_{ok}}\left[\Psi_{ok}^{\frac{2}{\varepsilon_{ok}}}\Gamma\left(-\frac{2}{\varepsilon_{ok}},\frac{sux\Psi_{ok}}{\gamma_k\Psi_{ok1}}\right)\right]}\right]}{x^{\frac{2}{\varepsilon_{ok}}+1}\mathrm{e}^{\frac{sux}{\gamma_k}}}dx}. \tag{35}
$$

where (a) is obtained by noting that

$$\left\{I_o + I_c + \eta < \max_{i=1,\cdots,K} \gamma_i M_i\right\} = \left\{\frac{1}{\kappa} \times \max_{i=1,\cdots,K} \gamma_i M_i + \eta < I_o + I_c + \eta < \max_{i=1,\cdots,K} \gamma_i M_i\right\} \bigcup \left\{\left\{I_o + I_c + \eta < \max_{i=1,\cdots,K} \gamma_i M_i\right\} \bigcap \left\{I_o + I_c + \eta \leq \frac{\max_{i=1,\cdots,K} \gamma_i M_i}{\kappa} + \eta\right\}\right\},$$

and the second set in the union of two sets shown above is a null set, (b) expresses the probability of the coverage event in terms of the joint p.d.f., (c) is obtained by substituting for the joint p.d.f. from (27), then interchanging the order of integrations of the variables x and ω which is justified by the boundedness of the integrals. Finally, the above expression can be further simplified to obtain (4).

The same steps can be followed for obtaining (5), and are omitted for brevity.

B. Proof for Lemma 1

Given a BS belonging to the k^{th} open-access tier is at a distance R from the origin, then, due to [2, Theorem 2], $\tilde{R} = (P_{ok}\Psi_{ok})^{-1} R^{\varepsilon_{ok}}$ represents the distance of the BS from the origin where the BS arrangement is according to a non-homogeneous 1-D Poisson point process with BS density function $\tilde{\lambda}_{ok}(r)$, as long as $\mathbb{E}\left[\Psi_{ok}^{\frac{2}{\varepsilon_{ok}}}\right] < \infty$, for each $k = 1, 2, \cdots, K$. Similarly, for the closed-access tier, $\hat{R} = (P_c\Psi_c)^{-1} R^{\varepsilon_c}$ is the distance where the BS arrangement is according to a non-homogeneous 1-D Poisson point process with BS density function $\hat{\lambda}(r)$, as long as $\mathbb{E}\left[\Psi_c^{\frac{2}{\varepsilon_c}}\right] < \infty$. This is a consequence of the Mapping theorem [32, Page 18] and the Marking Theorem [32, Page 55] of the Poisson processes. Further, since the BS arrangements in the different tiers were originally independent of each other, the set of all the BSs in the equivalent 1-D non-homogeneous Poisson process is merely the union of all $\tilde{R}'s$ in all tiers. By the Superposition Theorem [32, Page 16] of Poisson processes, the combined process is a non-homogeneous Poisson point process with density function $\tilde{\lambda}(r) = \sum_{k=1}^{K} \tilde{\lambda}_{ok}(r)\,,\ r \geq 0$.

In summary, we have converted the BS arrangement on a 2-D plane of a HetNet to a BS arrangement of the equivalent 2-tier network along 1-D (positive x-axis), and hence, the SINR distributions of both these networks are also equivalent. Further, by our construction, the MIRP BS in the HetNet corresponds to the BS that is nearest to the origin (MS) in the equivalent 2-tier network. As a result, SINR may be written in terms of the $\tilde{R}$'s and $\hat{R}$'s indexed in the ascending order, and we get (10).

C. Proof for Lemma 2

The HetNet SINR under MIRP can be computed as follows. For each tier $m = 1, \cdots, K$, c (c refers to the closed-access tier), form the set $\left\{\left(P_{om}\Psi_{om,l}\right)^{-\frac{1}{\varepsilon}} R_{om,l}\right\}_{l=1}^{\infty}$ and represent as $\left\{\bar{R}_{m,l}\right\}_{l=1}^{\infty}$ where $\bar{R}$'s are ascendingly ordered. Now, $\left\{\bar{R}_{m,l}^{-\varepsilon}\right\}_{l=1}^{\infty}$ represents the received powers of all the m^{th} tier BSs in the descending order. Finally, the desired BS's power and tier index (T) can be easily found by identifying the maximum in the set $\left\{\bar{R}_{m,1}^{-\varepsilon}\right\}_{m=1}^{K}$ and the SINR can be computed. Using [19, Corollary 3] which is an application of the Marking theorem [32, Page 55], it can be seen that $\left\{\bar{R}_{m,l}\right\}_{l=1}^{\infty}$ represents the distances from origin of BSs arranged according to homogeneous Poisson point process with BS density $\lambda_{om} P_{om} \mathbb{E}\left[\Psi_{om}^{\frac{2}{\varepsilon}}\right]$, where Ψ_{om} has the same distribution as the m^{th} tier fading factors. As a result, the set $\left\{\bar{R}_{m,l}^{-\varepsilon}\right\}_{m=1,\ l=1}^{m=K,\ l=\infty}$ represents the set of received powers at the origin of the HetNet composed of K open-access tiers and a closed-acess tier with BS densities $\left\{\lambda_{ok} P_{ok} \mathbb{E}\left[\Psi_{ok}^{\frac{2}{\varepsilon}}\right]\right\}_{k=1}^{K}$, $\lambda_c P_c \mathbb{E}\left[\Psi_c^{\frac{2}{\varepsilon}}\right]$, respectively, with unity transmit powers and fading factors at each BS. This is equivalent to the original heterogeneous network and has the same SINR distribution, hence proving (11).

Further, using the Superposition theorem [32, Page 16], the K open-access tiers of the equivalent HetNet can be combined to form a single tier network with a BS density equal to $\sum_{k=1}^{K} \lambda_{ok} P_{ok}^{\frac{2}{\varepsilon}} \mathbb{E}\Psi_{ok}^{\frac{2}{\varepsilon}}$, thus proving the SINR equivalence in (12). The distribution of SINR of this two-tier network is the same as that of an MS in another two-tier network where the open-access tier has unity BS density, the closed-access tier has a BS density $\frac{\lambda_c P_c \mathbb{E}\left[\Psi_c^{\frac{2}{\varepsilon}}\right]}{\sum_{k=1}^{K} \lambda_{ok} P_{ok}^{\frac{2}{\varepsilon}} \mathbb{E}\Psi_{ok}^{\frac{2}{\varepsilon}}}$, unity transmit power and fading factors at all BSs and a background noise $\frac{\eta}{\left(\sum_{k=1}^{K} \lambda_{ok} P_{ok}^{\frac{2}{\varepsilon}} \mathbb{E}\Psi_{ok}^{\frac{2}{\varepsilon}}\right)^{-\frac{\varepsilon}{2}}}$, due to [19, Lemma 3] and hence we get the relation (13).

D. Proof for Theorem 3

From Corollary 1 and Lemma 1, we get the following stochastic equivalence:

$$\mathrm{SINR}_{T,I} =_{\text{st}} \left.\frac{h_{T,I}\tilde{R}_{T,I}^{-1}}{\sum_{\substack{k=1}}^{K}\sum_{\substack{(k,l)\neq(T,I)}}^{\infty} h_{kl}\tilde{R}_{kl}^{-1} + \sum_{l=1}^{\infty} g_l \hat{R}_l^{-1} + \eta}\right|_{\left(\{\tilde{\lambda}_k(r)\}_{k=1}^{\infty}, \hat{\lambda}(r)\right)},$$

where h_{kl}'s and g_l's are i.i.d. unit mean exponential random variables, $I = \underset{k=1,2,\cdots}{\operatorname{argmax}}\ h_{T,k}\tilde{R}_{T,k}^{-1}$, $\left\{\tilde{R}_{kl}\right\}_{l=1}^{\infty}$ and $\left\{\hat{R}_l\right\}_{l=1}^{\infty}$ are from non-homogeneous 1-D Poisson processes with density functions $\tilde{\lambda}_{ok}(r) = \lambda_{ok}\frac{2\pi}{\varepsilon_{ok}} P_{ok}^{\frac{2}{\varepsilon_{ok}}} r^{\frac{2}{\varepsilon_{ok}}-1}$, $k = 1, \cdots, K$ and $\hat{\lambda}(r) = \lambda_c \frac{2\pi}{\varepsilon_c} P_c^{\frac{2}{\varepsilon_c}} r^{\frac{2}{\varepsilon_c}-1}$, respectively. The following steps

derive the HetNet coverage probability and closely follows the proof techniques for [2, Theorem 4] and [26, Theorem 1]

$$\mathbb{P}^{\text{max-SINR}}_{\text{coverage}} = \mathbb{P}^{\text{MIRP}}_{\text{coverage}} = \sum_{i=1}^{K} \mathbb{P}\left(\left\{\frac{h_{ij}\tilde{R}_{ij}^{-1}}{\sum_{\substack{k=1\\(k,l)\neq(i,j)}}^{K}\sum_{l=1}^{\infty} h_{kl}\tilde{R}_{kl}^{-1} + \sum_{l=1}^{\infty} g_l \hat{R}_l^{-1} + \eta} > \beta_i\right\}\right)$$

$$\overset{(a)}{=} \sum_{i=1}^{K} \mathbb{E}_{\tilde{R}_{ij}}\left[\mathrm{e}^{-\beta_i \tilde{R}_{ij}\eta}\mathbb{E}\left[\mathrm{e}^{-\beta_i \tilde{R}_{ij}\sum_{\substack{k=1\\(k,l)\neq(i,j)}}^{K}\sum_{l=1}^{\infty} h_{kl}\tilde{R}_{kl}^{-1}}\middle|\tilde{R}_{ij}\right]\times \mathbb{E}\left[\mathrm{e}^{-\beta_i \tilde{R}_{ij}\sum_{l=1}^{\infty} g_l \hat{R}_l^{-1}}\middle|\tilde{R}_{ij}\right]\right]$$

$$\overset{(b)}{=} \sum_{i=1}^{K}\int_{r=0}^{\infty} \tilde{\lambda}_{oi}(r)\,\mathrm{e}^{-\eta\beta_i r - \frac{\lambda_c \pi (P_c \beta_i r)^{\frac{2}{\varepsilon_c}} \mathbb{E}\left[\Psi_c^{\frac{2}{\varepsilon_c}}\right]}{\Gamma\left(1+\frac{2}{\varepsilon_c}\right)\mathrm{sinc}\left(\frac{2\pi}{\varepsilon_c}\right)}} \times \mathrm{e}^{-\sum_{l=1}^{K} \frac{\lambda_{ol}\pi (P_{ol}\beta_i r)^{\frac{2}{\varepsilon_{ol}}} \mathbb{E}\left[\Psi_{ol}^{\frac{2}{\varepsilon_{ol}}}\right]}{\Gamma\left(1+\frac{2}{\varepsilon_{ol}}\right)\mathrm{sinc}\left(\frac{2\pi}{\varepsilon_{ol}}\right)}} dr,$$

where $\tilde{R}_{ij}$ is the distance from the origin of an arbitrary point in the non-homogeneous Poisson process with density function $\tilde{\lambda}_{oi}(r)$, (a) is obtained by computing the coverage probability w.r.t. h_{ij} conditioned on all the other involved random variables and noting that the two Poisson processes are independent of each other, (b) is obtained by evaluating the inner expectations by applying Campbell's theorem [32] (same steps as in the proof of [2, Theorem 4]) and expressing the expectation w.r.t. $\tilde{R}_{ij}$ by the integral where $\tilde{\lambda}(r)\,dr$ is the probability that there exists a point in the interval $(r, r+dr)$, and finally (16) is obtained by simplifying the integral in (b).

E. Proof for Theorem 4

The HetNet coverage probability is given in (36), shown at the bottom of the page, where (a) is from the stochastic equivalence in Corollary 5, (b) is obtained due to the independence of each tier in the HetNet given (T, R_{oT1}). Now, we derive expressions for E_1 and E_2 in (b):

$$E_1 = \exp\left(-\int_{r=0}^{\infty}\left(1-\mathbb{E}_{\Psi_c}\left[\mathrm{e}^{\frac{-\beta_k \tilde{R}_{ok1}\Psi_c}{\tilde{P}_{ok1} r}}\right]\right)\hat{\lambda}(r)\,dr\right)$$

$$= \mathrm{e}^{-\frac{\lambda_c \pi \left(P_c \beta_k \tilde{R}_{ok1}\right)^{\frac{2}{\varepsilon_c}}}{\tilde{P}_{ok1}^{\frac{2}{\varepsilon_c}}\mathrm{sinc}\left(\frac{2\pi}{\varepsilon_c}\right)}},$$

$$E_2 = e^{-\int_{r=\tilde{R}_{ok1}}^{\infty}\left(1-\mathbb{E}_{\Psi_{om}}\left[\mathrm{e}^{\frac{-\beta_k \tilde{R}_{ok1}\Psi_{om}}{\tilde{P}_{ok1} r}}\right]\right)\tilde{\lambda}_{om}(r)dr}$$

$$= \mathrm{e}^{-\lambda_{om}\pi \frac{2\beta_k \left(P_{om} B_{om} \tilde{R}_{ok1}\right)^{\frac{2}{\varepsilon_{om}}}}{\tilde{P}_{ok1}(\varepsilon_{om}-2)}} \times {}_2F_1\left(1,1-\frac{2}{\varepsilon_{om}};2-\frac{2}{\varepsilon_{om}};-\frac{\beta_k}{\tilde{P}_{ok1}}\right).$$

Finally, (23) is obtained by computing each expectation in (b) by applying the Campbell-Mecke theorem. For $\{\varepsilon_{ok}\}_{k=1}^{K} = \varepsilon$ and $\eta = 0$, the integral in (23) simplifies to (24).

F. Simulation Method

The k^{th} tier of the HetNet with K tiers is identified by the following set of system parameters: $(\lambda_k,\ P_k,\ \Psi_k,\ \varepsilon_k,\ \beta_k)$, where the symbols have all been defined in Section II, and $k = 1,\ 2, \cdots,\ K$, where K is the total number of tiers. Now we illustrate the steps for simulating the HetNet in order to obtain the SINR distribution and the coverage probability assuming the MS is at the origin. The algorithm for the Monte-Carlo simulation is as follows: 1) Generate N_k random variables according to a uniform distribution in the circular region of radius R_B for the locations of all the k^{th} tier BSs, where $N_k \sim \text{Poisson}\left(\lambda_k \pi R_B^2\right)$. 3) Compute the SINR at the desired BS according to Section II-C and record the tier index I of the desired BS. Repeat the same procedure T (typically, >50000) times. Finally, the tail probability of SINR at η is given by $\frac{\{\#\text{ of trials where SINR} > \eta\}}{T}$, and the coverage probability is given by $\sum_{k=1}^{K}\frac{\{\#\text{ of trials where } I=k \text{ and } SINR>\beta_k\}}{T}$.

$$\mathbb{P}^{\text{MBRP}}_{\text{coverage}} \overset{(a)}{=} \sum_{k=1}^{K}\mathbb{E}_{T,\tilde{R}_{oT1}}\left[\left\{\frac{\tilde{P}_{ok1}\Psi_{ok1}\tilde{R}_{ok1}^{-1}}{\sum_{n=1}^{\infty}\frac{\Psi_{cn}}{\hat{R}_{cn}} + \eta + \sum_{\substack{m=1\\(m,l)\neq(k,1)}}^{K}\sum_{l=1}^{\infty}\frac{\tilde{P}_{oml}\Psi_{oml}\mathcal{I}\left(\tilde{R}_{oml}>\tilde{R}_{ok1}\right)}{\tilde{R}_{oml}}} > \beta_T\right\}\middle| k, \tilde{R}_{ok1}\right]$$

$$\overset{(b)}{=} \sum_{k=1}^{K}\mathbb{E}_{T,\tilde{R}_{oT1}}\left[\mathrm{e}^{-\frac{\eta\beta_k\tilde{R}_{ok1}}{\tilde{P}_{ok1}}} \times \underbrace{\mathbb{E}\left[\prod_{n=1}^{\infty}\mathrm{e}^{\frac{-\beta_k\tilde{R}_{ok1}\Psi_{cn}}{\tilde{P}_{ok1}\hat{R}_{cn}}}\middle| T=k,\ \tilde{R}_{oT1}=\tilde{R}_{ok1}\right]}_{=E_1}\right.$$

$$\left.\times \prod_{m=1}^{K}\underbrace{\mathbb{E}\left[\prod_{l=1}^{\infty}\mathrm{e}^{\frac{-\beta_k\tilde{R}_{ok1}\Psi_{oml}}{\tilde{P}_{ok1}\tilde{R}_{oml}}\mathcal{I}\left(\tilde{R}_{oml}>\tilde{R}_{ok1}\right)}\middle| T=k,\ \tilde{R}_{oT1}=\tilde{R}_{ok1}\right]}_{=E_2}\right] \tag{36}$$

REFERENCES

[1] P. Madhusudhanan, J. G. Restrepo, Y. Liu, T. X. Brown, and K. Baker, "Multi-tier network performance analysis using a shotgun cellular system," in *Proc. IEEE Wireless Commun. Symp. (GLOBECOM'110)*, Dec. 2011, pp. 1–6.

[2] P. Madhusudhanan, J. Restrepo, Y. Liu, and T. Brown, "Downlink coverage analysis in a heterogeneous cellular network," in *Proc. IEEE Global Commun.Conf. (GLOBECOM)*, Dec. 2012, pp. 4170–4175.

[3] H. S. Dhillon, R. K. Ganti, and J. G. Andrews, "Load-aware modeling and analysis of heterogeneous cellular networks," *IEEE Trans. Wireless Commun.*, vol. 12, no. 4, pp. 1666–1677, Apr. 2013 [Online]. Available: http://ieeexplore.ieee.org/stamp/stamp.jsp?tp=&arnumber=6463498&isnumber=6507664

[4] S.-P. Yeh, S. Talwar, G. Wu, N. Himayat, and K. Johnsson, "Capacity and coverage enhancement in heterogeneous networks," *IEEE Wireless Commun.*, vol. 18, no. 3, pp. 32–38, Jun. 2011.

[5] A. Damnjanovic *et al.*, "A survey on 3GPP heterogeneous networks," *IEEE Wireless Commun.*, vol. 18, no. 3, pp. 10–21, Jun. 2011.

[6] A. Damnjanovic, J. Montojo, J. Cho, H. Ji, J. Yang, and P. Zong, "UE's rolein LTE advanced heterogeneous networks," *IEEE Commun. Mag.*, vol. 50, no. 2, pp. 164–176, Feb. 2012.

[7] 4G Americas Report, "4G mobile broadband evolution: 3GPP release 10 and beyond," white paper, Feb. 2011.

[8] Qualcomm, "LTE advanced: Heterogeneous network," white paper, Jan. 2011.

[9] V. Chandrasekhar, J. Andrews, and A. Gatherer, "Femtocell networks: A survey," *IEEE Commun. Mag.*, vol. 46, no. 9, pp. 59–67, Sep. 2008.

[10] X. Lagrange, "Multitier cell design," *IEEE Commun. Mag.*, vol. 35, no. 8, pp. 60–64, Aug. 1997.

[11] M. Haenggi and R. K. Ganti, *Interference in Large Wireless Networks*. Hanover, MA, USA: NoW Publishers Inc., 2008, vol. 3.

[12] F. Baccelli and B. Błaszczyszyn, *Stochastic Geometry and Wireless Networks, Volume I–Theory*. Hanover, MA, USA: NoW Publishers, 2009, vol. 3.

[13] F. Baccelli and B. Błaszczyszyn, *Stochastic Geometry and Wireless Networks, Volume II–Applications*. Hanover, MA, USA: NoW Publishers, 2009, vol. 4.

[14] V. M. Nguyen and F. Baccelli, "A stochastic geometry model for the best signal quality in a wireless network," in *Proc. 8th Int. Symp. Model. Optim. Mobile Ad Hoc Wireless Netw. (WiOpt)*, May 2010, pp. 465–471.

[15] T. X. Brown, "Analysis and coloring of a shotgun cellular system," in *Proc. IEEE Radio Wireless Conf. (RAWCON'98)*, Aug. 1998, pp. 51–54.

[16] T. Brown, "Cellular performance bounds via shotgun cellular systems," *IEEE J. Sel. Areas Commun.*, vol. 18, no. 11, pp. 2443–2455, Nov. 2000.

[17] J. Andrews, F. Baccelli, and R. Ganti, "A tractable approach to coverage and rate in cellular networks," *IEEE Trans. Commun.*, vol. 59, no. 11, pp. 3122–3134, Nov. 2011.

[18] P. Madhusudhanan, J. Restrepo, Y. Liu, and T. Brown, "Carrier to interference ratio analysis for the shotgun cellular system," in *Proc. IEEE Global Telecommun. Conf. (GLOBECOM'09)*, Nov. 2009, pp. 1–6.

[19] P. Madhusudhanan, J. Restrepo, Y. Liu, T. Brown, and K. Baker, "Downlink performance analysis for a generalized shotgun cellular system," *IEEE Trans. Wireless Commun.*, vol. 13, no. 12, pp. 6684–6696, Dec. 2014.

[20] P. Madhusudhanan, J. G. Restrepo, Y. E. Liu, T. X. Brown, and K. R. Baker, "Stochastic ordering based carrier-to-interference ratio analysis for the shotgun cellular systems," *IEEE Wireless Commun. Lett.*, vol. 1, no. 6, pp. 565–568, Dec. 2012.

[21] B. Błaszczyszyn, M. K. Karray, and H. P. Keeler, "Using poisson processes to model lattice cellular networks," in *Proc. IEEE INFOCOM*, Apr. 2013, pp. 773–781.

[22] S. Mukherjee, "Downlink SINR distribution in a heterogeneous cellular wireless network with biased cell association," in *Proc. IEEE 1st Int. Workshop Small Cell Wireless Netw. (ICC)*, 2012, pp. 6780–6786.

[23] S. Mukherjee, "Distribution of downlink SINR in heterogeneous cellular networks," *IEEE J. Sel. Areas Commun.*, vol. 30, no. 3, pp. 575–585, Apr. 2012.

[24] S. Mukherjee, "Downlink SINR distribution in a heterogeneous cellular wireless network with max-SINR connectivity," in *Proc. 49th Annu. Allerton Conf. Commun. Control Comput. (Allerton)*, Sep. 2011, pp. 1649–1656.

[25] S. Mukherjee, "Analysis of UE outage probability and macrocellular traffic offloading for WCDMA macro network with femto overlay under closed and open access," in *Proc. IEEE Int. Conf. Commun. (ICC)*, Jun. 2011, pp. 1–6.

[26] H. S. Dhillon, R. K. Ganti, F. Baccelli, and J. G. Andrews, "Modeling and analysis of K-tier downlink heterogeneous cellular networks," *IEEE J. Sel. Areas Commun.*, vol. 30, no. 3, pp. 550–560, Apr. 2012.

[27] H. S. Dhillon, R. K. Ganti, F. Baccelli, and J. G. Andrews, "Coverage and ergodic rate in K-tier downlink heterogeneous cellular networks," in *Proc. 49th Annu. Allerton Conf. Commun. Control Comput. (Allerton)*, Sep. 2011, pp. 1627–1632.

[28] H. Dhillon, R. Ganti, and J. Andrews, "A tractable framework for coverage and outage in heterogeneous cellular networks," in *Proc. Inf. Theory Appl. Workshop(ITA)*, Feb. 2011, pp. 1–6.

[29] H. Dhillon, R. Ganti, and J. Andrews, "Load-aware modeling and analysis of heterogeneous cellular networks," *IEEE Trans. Wireless Commun.*, vol. 12, no. 4, pp. 1666–1677, Apr. 2013.

[30] H.-S. Jo, Y. J. Sang, P. Xia, and J. Andrews, "Heterogeneous cellular networks with flexible cell association: A comprehensive downlink SINRnalysis," *IEEE Trans. Wireless Commun.*, vol. 11, no. 10, pp. 3484–3495, Oct. 2012.

[31] P. Xia, V. Chandrasekhar, and J. Andrews, "Open vs. closed access femtocells in the uplink," *IEEE Trans. Wireless Commun.*, vol. 9, no. 12, pp. 3798–3809, Dec. 2010.

[32] J. F. C. Kingman, *Poisson Processes (Oxford Studies in Probability)*. London, U.K.: Oxford Univ. Press, Jan. 1993.

[33] A. M. Mathai and H. J. Haubold, *Special Functions for Applied Scientists*. New York, NY, USA: Springer, Mar. 2008.

Prasanna Madhusudhanan received the B.E. degree in telecommunication engineering from Visvesvaraya Technological University, Belgaum, India, in 2006, and the M.S. and Ph.D. degrees from the Department of Electrical, Computer, and Energy Engineering, University of Colorado at Boulder, Boulder, CO, USA, in 2010 and 2013, respectively. Since September 2013, he has been working with Qualcomm Inc., Boulder, CO, USA. His research interests include communication theory, wireless networks, stochastic geometry, and dynamical systems.

Juan G. Restrepo received the B.S. degree in physics from the University of the Andes, Bogotá, Colombia, in 1999, and the Ph.D. degree in applied mathematics from the University of Maryland, College Park, MD, USA, in 2005. He is an Assistant Professor with the Department of Applied Mathematics, University of Colorado at Boulder, Boulder, CO, USA. His research interests include dynamical systems, chaos, synchronization of coupled oscillators, dynamics on complex networks, and cardiac dynamics.

Youjian Liu (S'98–M'01) received the B.E. degree in electrical engineering from Beijing University of Aeronautics and Astronautics, Beijing, China, in 1993, the M.S. degree in electronics from Beijing University, China, in 1996, and the M.S. and Ph.D. degrees in electrical engineering from The Ohio State University, Columbus, OH, USA, in 1998 and 2001, respectively. He joined the Department of Electrical and Computer Engineering, University of Colorado at Boulder, Boulder, CO, USA, in August 2002, where he is currently an Associate Professor. From January 2001 to August 2002, he worked on space-time communications for 3G mobile communication systems as a Member of the Technical Staff with CDMA System Analysis and Algorithms Group, Wireless Advanced Technology Laboratory, Lucent Technologies, Bell Labs Innovations, Whippany, NJ, USA. His research interests include network communications, information theory, and coding theory.

Timothy X Brown received the B.S. degree in physics from Pennsylvania State University, State College, PA, USA, and the Ph.D. degree in electrical engineering from California Institute of Technology, Pasadena, CA, USA. He is a Professor with Carnegie Mellon University, Kigali, Rwanda. He is also a Professor with the University of Colorado at Boulder, Boulder, CO, USA, most recently as the Director of the Interdisciplinary Telecommunications Program. His research interests include cybersecurity, spectrum policy, and wireless networks. He was a recipient of the NSF CAREER Award and the GWEC Wireless Educator of the Year Award.